

1 **Embracing fine-root system complexity to improve the predictive understanding of**
2 **ecosystem functioning**

3

4 Bin Wang¹, M. Luke McCormack², Daniel M. Ricciuto¹, Xiaojuan Yang¹, and Colleen M. Iversen¹

5

6 1 Environmental Sciences Division, Oak Ridge National Laboratory, Oak Ridge, Tennessee 37830
7 USA

8 2 Center for Tree Science, The Morton Arboretum, Lisle, Illinois 60532 USA

9

10 Notice: This manuscript has been authored by UT-Battelle, LLC, under contract DE-AC05-
11 00OR22725 with the US Department of Energy (DOE). The US government retains and the
12 publisher, by accepting the article for publication, acknowledges that the US government retains a
13 nonexclusive, paid-up, irrevocable, worldwide license to publish or reproduce the published form
14 of this manuscript, or allow others to do so, for US government purposes. DOE will provide public
15 access to these results of federally sponsored research in accordance with the DOE Public Access
16 Plan (<http://energy.gov/downloads/doe-public-access-plan>).

17

18 **Abstract**

19 Projecting the functioning of the biosphere requires a holistic consideration of whole-ecosystem
20 processes. Although improving leaf and canopy processes has been the focus of ecosystem model
21 development since the 1970s, the arbitrary homogenization of fine-root systems into a single pool
22 is at odds with observations. This discrepancy has increased in the last two decades as accelerated
23 conceptual and empirical advances have revealed functional differentiation and cooperation

24 conferred by the hierarchical structure of fine-root orders and associations with mycorrhizal fungi
25 in fine-root systems. To close this model-data gap, we propose a 3-pool structure comprising
26 Transport and Absorptive fine roots with Mycorrhizal fungi (TAM) to model vertically resolved
27 fine-root systems across organizational and spatial-temporal scales. A comparison of TAM to the
28 single fine-root structure in a state-of-the-art Earth System Model using the ‘big-leaf’ approach
29 demonstrates robust impacts on carbon cycling in temperate forests, lending further quantitative
30 support to the empirical and theoretical basis for TAM. Strong support in both theory and practice
31 therefore suggests a move beyond the useful but incorrect paradigm of single-pool
32 homogenization, echoing a broad trend of embracing ecological complexities in terrestrial
33 ecosystem modelling. Although challenges lay ahead towards realizing TAM in ecologically
34 realistic demography models simulating emergent functioning from pattern and diversity, adoption
35 of TAM by both modelers and empiricists holds promise to build a better predictive understanding
36 of ecosystem functioning in the context of global change.

37

38 **Key words:** ecosystem model, complexity, fine root, mycorrhiza, TAM, partitioning, phenology,
39 demography

40

41 **1. Introduction**

42 Earth System Models (ESMs) grapple with low confidence in projecting the functioning of
43 the biosphere within the Earth System across space and over time. Many efforts have been made
44 to improve predictability regarding the structure and functions of terrestrial ecosystems since the
45 1970s, though this work has mostly focused on the aboveground leaf and canopy processes (e.g.,
46 **Sinclair et al., 1976; Friend et al. 2014; Lovenduski and Bonan 2017**). Meanwhile, plant roots

47 have been integral to the evolution of plant form and function (e.g., **Raven and Edwards 2001**)
48 and sit at the nexus of plant-microbe-soil interactions in the biosphere, linking the atmosphere and
49 pedosphere (e.g., **Bardgett et al. 2014; Freschet et al. 2021**). However, current models treat fine-
50 root systems—the ephemeral portion of the root system responsible for water and nutrient
51 acquisition—rudimentarily, and more importantly, lag behind empirical and theoretical advances
52 with regard to fine-root system complexity (e.g., **Fitter 1982; Pregitzer 2002; Phillips et al. 2013;**
53 **McCormack et al. 2015a**). This model-data discrepancy likely contributes to the poor
54 representation of terrestrial ecosystem feedbacks to increasing CO₂ within ESMs (e.g., **Warren et**
55 **al. 2014; Bonan and Doney 2018**). Therefore, embracing fine-root system complexity to improve
56 structural realism is expected to increase the prognostic capability of terrestrial ecosystem models
57 in biosphere-atmosphere interactions.

58 Over the past two decades belowground ecologists have made tremendous progress in
59 revealing the heterogeneity within fine-root systems. Within a fine-root system, plants have
60 evolved roots with unique morphological, anatomical, chemical, and physiological features that
61 differ among root branching orders (e.g., **Pregitzer et al. 2002; Atucha et al. 2021**), as well as
62 varying microbial associations with both mycorrhizal fungi and bacteria (e.g., **Sen and Jenik**
63 **1962; King et al. 2021**). These structural differences support both functional differentiation and
64 cooperation within fine-root systems; fine roots of higher orders are primarily responsible for
65 transport of water and nutrients to the rest of the plant, while finer and more distal roots in
66 cooperation with mycorrhizal fungi are responsible for nutrient and water absorption (e.g., **Hishi**
67 **& Takeda 2005; McCormack et al. 2015a; Wang et al. 2022**). This heterogeneity, and degree
68 of coordination with aboveground plant activities, changes with species and habitat, forming

69 diverse whole-plant strategies across biomes under physical and functional constraints (e.g.,
70 **McCormack and Iversen 2019; Weigelt et al. 2021**).

71 By contrast, fine-root systems in ecosystem models are often treated without accounting
72 for their structural and functional heterogeneity. Currently, the prevailing option in terrestrial
73 ecosystem modelling remains a single fine-root pool (e.g., **Kleidon & Heimann 1998; Zeng 2001;**
74 **Warren et al. 2015; Burrows et al. 2020**). Although empiricists have advocated for specifically
75 representing arbuscular mycorrhizal fungi traits and function (**Treseder 2016**) and modelers have
76 even already incorporated impacts of mycorrhizal fungi into models either implicitly (e.g.,
77 **Woodward and Smith 1994; Brzostek et al. 2014**) or explicitly (e.g., **Hunt et al. 1991; Orwin**
78 **et al. 2011; Sulman et al. 2018**), no efforts yet holistically integrate the complexity of fine-root
79 system with a balanced perspective of both fine roots and mycorrhizal fungi. This
80 oversimplification of fine-root system structure fundamentally limits accurate representation of its
81 functioning and hence above- and below-ground interactions (e.g., **Smithwick et al. 2014;**
82 **Warren et al. 2015**). In addition, such a simplification forms an asynchronous development in
83 terrestrial ecosystem models relative to other components (notably photosynthesis and canopy
84 processes) that likely imparts a structural limit on improvements to whole model performance. For
85 instance, fine-root dynamics are normally assumed to follow leaf phenology closely (e.g.,
86 **Burrows et al. 2020**). Of course, there are individual-level plant models, especially for crops,
87 simulating explicit root structures (e.g., **Pointurier et al. 2021**). However, it has been a challenge
88 to integrate theoretical and empirical advances at scales relevant for ecosystem models while
89 balancing model simplicity and realism.

90 Such a large model-theory discrepancy raises the question of whether models can improve
91 performance with an appreciation of fine-root system complexity. The core of this question about

92 a single pool versus a more explicit treatment, by analogy, mirrors the debates in vegetation
93 modelling on one layer versus multilayer canopy modelling (e.g., **Raupach and Finnigan 1988**),
94 on individual-based versus various functional group modelling (e.g., **Smith et al. 1997; Shugart**
95 **et al. 2018**), and on different lumping approaches in modelling various complex physical,
96 chemical, and biological systems more generally (e.g., **Okino and Mavrovouniotis 1998**). For
97 example, comparisons of one- versus multi-layer canopy simulations have led to the conclusion
98 that land surface models should move beyond the useful but incorrect paradigm of single-layer
99 canopy scheme to help resolve uncertainties in canopy processes (**Bonan et al. 2021**). Similarly,
100 current models show large uncertainties related to belowground processes; for example, a
101 comprehensive sensitivity analysis of the ELM (**Box 1**) revealed large prediction uncertainty
102 arising from uncertainty in root-related parameters and processes (**Ricciuto et al. 2018**).
103 Constraining model uncertainty requires a model structure that can predict measurable quantities
104 in real fine-root systems. Furthermore, improving the representation of fine roots may help model
105 performance by identifying other coupled but deficient components. Therefore, dedicated efforts
106 are warranted to explore alternatives to the single fine-root pool in current terrestrial ecosystem
107 models. Meanwhile, the increasingly available data on fine-root traits (FRED; **Iversen et al. 2017**;
108 **Box 1**) and fungal traits (e.g., **Zanne et al. 2020; Iversen and McCormack 2021**) can facilitate
109 these efforts.

110 To this end, we propose a generalized 3-pool structure including Transport and Absorptive
111 fine roots as well as Mycorrhizal fungi (TAM) to represent fine-root systems across organizational
112 and spatio-temporal scales in terrestrial ecosystem models. This function-based TAM structure is
113 intended to approximate the high-dimensional heterogeneity within the hierarchical branching
114 fine-root systems and to serve as an explicit but tractable approach to model fine-root system

115 functioning. The overarching objective of this viewpoint is to argue for adoption of this structure
116 as the quantitative keystone of the bridge between modelers and empiricists. To achieve this
117 objective, we evaluate this TAM structure both theoretically and quantitatively. After elaborating
118 on the conceptual, theoretical, and empirical bases of TAM, we specifically address the following
119 three questions: First, how to realize TAM in ecosystem models? Second, how does this new
120 structure alter simulations of major ecosystem carbon fluxes (e.g., productivity and soil
121 respiration) and pools (e.g., fine-root biomass and soil carbon storage)? Third, what are the
122 uncertainties and challenges in broadly adopting this TAM structure?

123 We answer the first question by proposing a high-level framework of carbon partitioning,
124 the phenological patterns of root and fungal birth, growth, and death, and the vertical distribution
125 of fine roots and fungi throughout the soil profile that can be integrated into existing modelling
126 paradigms of varying complexity in terms of vegetation structure. Starting with the relatively
127 simple big-leaf modeling paradigm, we then answer the second question with an example
128 implementation in the context of a representative big-leaf model with a single fine-root pool—
129 ELM—in two different temperate forest types (deciduous and evergreen forests) across the Eastern
130 United States. For a proof-of-concept purpose the focus of this example is mostly descriptive rather
131 than analytical. By showing significant impacts of TAM in a relatively simple model structure we
132 do not fully address the question of whether TAM really improves model predictability. Rather,
133 we believe a combination of the conceptual, theoretical, and empirical bases and an initial
134 demonstration in this viewpoint lays the groundwork for broad adoption and evaluation of TAM
135 in different modelling paradigms against observations at varying scales. Accordingly, we answer
136 the third question by discussing uncertainties and challenges to fully exploit its potential. We

137 conclude by pointing out potential implications of TAM for guiding empirical research,
138 understanding ecosystem functioning, and improving ESMs prognosis.

139

140 **Box 1 Terminology**

141 **Fine-root system:** Root-mycorrhizal association at the individual plant level comprising fine roots
142 of different orders and associated mycorrhizal fungi.

143 **TAM:** An approach argued for in this viewpoint to abstract fine-root systems with two pools
144 representing the traits and function of fine roots—transport roots (T) and absorptive roots (A)—as
145 well as mycorrhizal fungi (M).

146 **FRED (Fine Root Ecology Database):** a database conceived and built by **Iversen et al. (2017)**
147 that houses fine-root trait observations from across the world (<https://roots.ornl.gov/>).

148 **ESM (Earth System Model):** A coupled-climate model that explicitly simulates the atmosphere,
149 the ocean, and the land surface in the Earth system, of which the land component is usually referred
150 to as the land model.

151 **Terrestrial Ecosystem Model:** Models that simulate ecosystems across spatial-temporal scales in
152 the terrestrial biosphere, which is synonymous with land model, terrestrial biosphere model, or
153 ecosystem model in this study.

154 **Big-leaf model:** Terrestrial ecosystem models that represent vegetation using prescribed, static
155 fractional coverage of different Plant Functional Types (an approach to aggregate and simplify
156 global plant diversity) with either a single canopy layer (i.e., one big-leaf model) or sun and shaded
157 layers (i.e., two big-leaf model).

158 **ELM:** The land model using the big-leaf approach with a single fine-root pool in the Energy
159 Exascale Earth System Model (E3SM), a state-of-the-art ESM developed by the US Department
160 of Energy (**Golaz et al. 2019**).

161 **Demography model:** Terrestrial ecosystem models that can simulate dynamics of vegetation
162 pattern (e.g., forested mosaic of gaps) with demographic processes of growth, mortality, and
163 reproduction.

164 **Demand-driven approach:** An approach for formulating nutrient uptake by fine-root systems of
165 plants or heterotrophic microbes based exclusively on their nutrient demands determined by their
166 potential growth or decomposition rates. The competition between plants and microbes for
167 nutrients is resolved by comparing their demands, which is thus referred to as relative-demand
168 approach.

169 **Trait divergence:** Trait variability or heterogeneity where a 3-pool TAM model allows for unique
170 trait values for each pool while a 1-pool fine-root model only allows a single value to represent
171 the fine-root system.

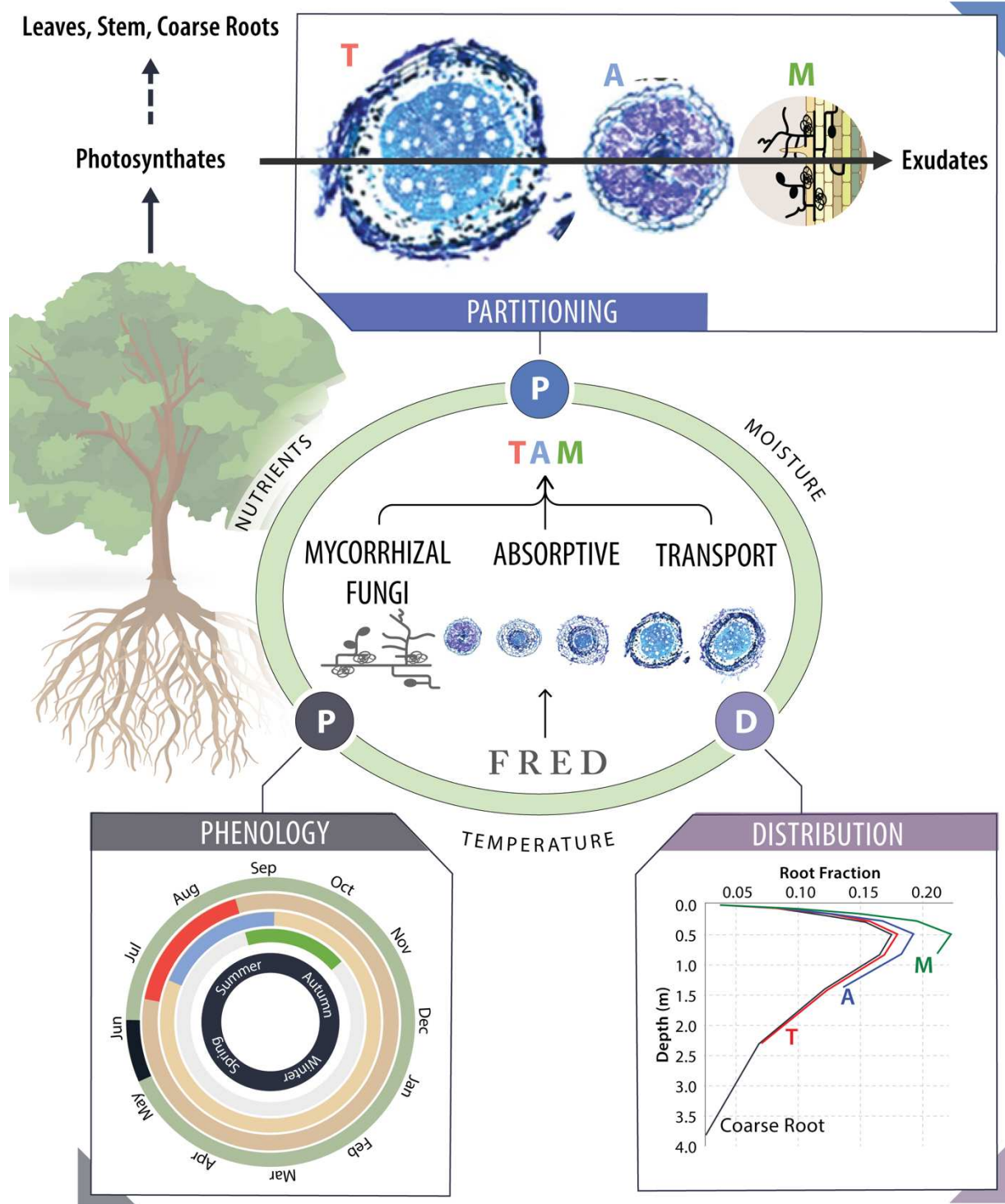
172 **Preservation:** A procedure to keep the same whole bulk fine-root system property (e.g., C/N in
173 this study) while capturing trait divergence from a 1-pool to 3-pool TAM structure.

174 **Partitioning:** The division of plant photosynthates allocated to one of the TAM pools.

175 **Distribution:** The explicit vertical representation of photosynthates in a soil profile partitioned to
176 one of the TAM pools.

177

178



180 **Fig. 1 Schematic of the 3-pool TAM structure governed by interrelated processes of**
181 **partitioning, phenology, and distribution under environmental constraints.** TAM is
182 conceived to be informed by order- or function-based explicit measurements of fine-root and
183 mycorrhizal fungal traits as compiled in various databases, e.g., FRED. Partitioning of
184 photosynthates to the outside of fine-root systems as exudates is also indicated, though not yet
185 explicitly treated in the current study. Asynchronous phenology within TAM and with leaf
186 phenology is illustrated with approximate periods of production (indicated by colored bands) for
187 leaves, T, A, and M pools based on a *Quercus alba* Plot at The Morton Arboretum, USA in 2019.
188 In addition, the different vertical distribution of TAM (in reference to the coarse root distribution)
189 is for an illustrative purpose only; distribution of new carbon still assumed to be the same across
190 TAM pools though with different turnover rates. The cross sections of 5 fine-root orders are
191 reproduced from **McCormack et al. (2015a)**.

192

193 **2. Conceptual, theoretical, and empirical basis of the TAM structure**

194 TAM arises from a conceptual shift of fine-root systems. Fine-root systems develop
195 structural and functional differentiation within an individual plant and express substantial variation
196 among individuals, across species, and across biomes (e.g., **Weigelt et al. 2021**). Structurally, fine-
197 root systems bear a hierarchical branching structure with different orders; each order displays
198 different properties in its anatomy, morphology, chemistry, physiology, lifespan, and fungal
199 colonization (e.g., **Pregitzer et al. 2002; Guo et al., 2008; McCormack et al., 2017; Klimešová**
200 **& Herben 2021; Zhou et al. 2022**). This structural variation underlies distinct functional
201 differentiation within fine-root systems. Therefore, an arbitrary homogenization of such
202 differentiation below the 2-mm diameter threshold as functionally equivalent fine roots is

203 problematic. Instead, a new conceptualization of functional differentiation is argued in terms of
204 transport (coarser, high-order fine roots), absorption (finer, low-order fine roots), and facilitation
205 by colonizing mycorrhizal fungi (**McCormack et al 2015a**). Therefore, following a long tradition
206 of function-based lumping of objects in both empirical and quantitative ecology (e.g., **Raunkiaer**
207 **1934**; **Root 1967**; **Grime 1974**; **Smith et al. 1997**), we aggregate fine-root systems of different
208 orders and associations with mycorrhizal fungi into three functional pools that comprise transport
209 roots, absorptive roots, and mycorrhizal fungi—TAM (**Fig.1**).

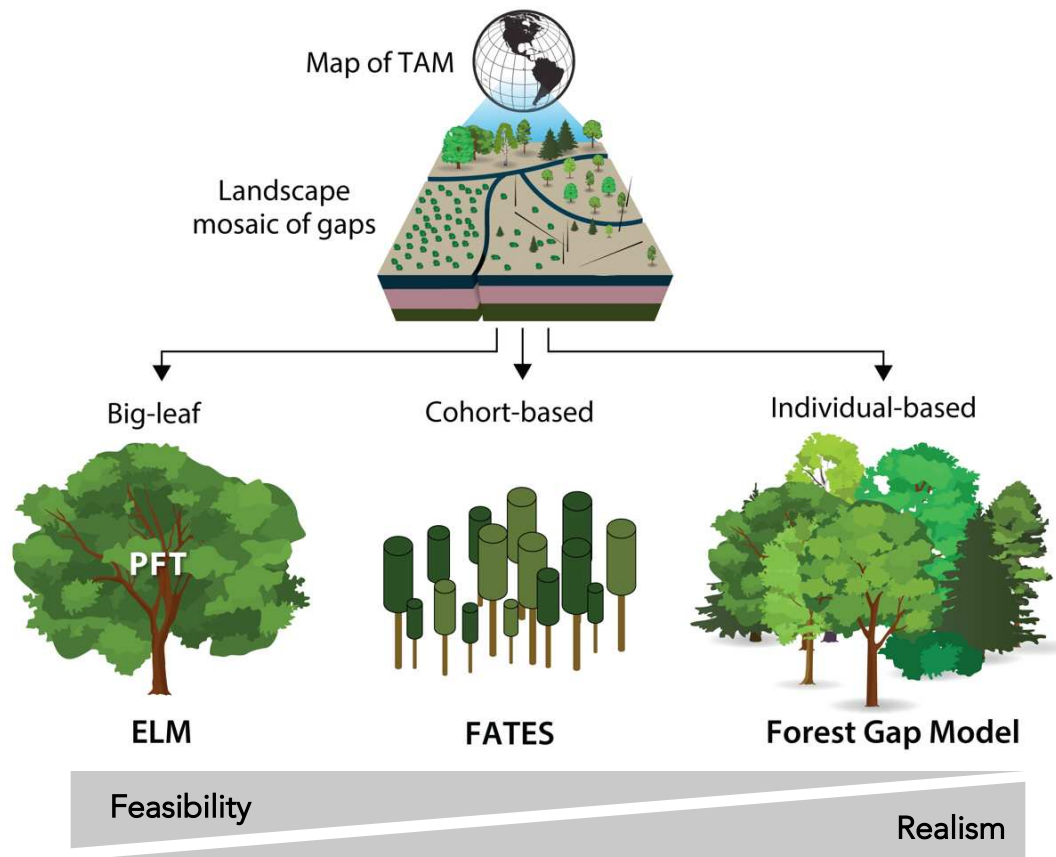
210 Theoretically, this 3-pool TAM structure allows a balanced perspective of fine roots and
211 fungi in ecosystem models while capturing both functional differentiation and cooperation within
212 the fine-root systems. A single fine-root pool oversimplifies fine-root systems and misses
213 important symbiotic associations with mycorrhizal fungi. Recognizing the importance of
214 mycorrhizal fungi, some models have accounted for these fine-root partners as an implicit
215 component (e.g., **Koide and Elliot 1989**; **Kirschbaum and Paul 2002**; **Brzostek et al. 2014**).
216 While these efforts have contributed to more accurate simulations of vegetation nutrient uptake
217 and soil organic matter decomposition in general, these plant-centric models do not include an
218 active mycorrhizal pool that enables a balanced perspective of plant and mycorrhizal fungi.
219 However, even when an explicit mycorrhizal fungal pool is included (e.g., **Hunt et al. 1991**;
220 **Orwin et al. 2011**; **Sulman et al. 2019**), a homogenous treatment of fine roots still misses the
221 structural and functional differentiation arising from fine-root orders (**Fig.1**). Of course, a
222 discretized 3-pool structure cannot fully capture the high-dimensional fine-root system
223 heterogeneity (typically five or more root orders plus mycorrhizal fungal colonization, e.g.,
224 **Pregitzer et al. 2002**; **Guo et al. 2008**). Individual-level plant models, especially for crops, may
225 be suitable for an order-based continuous treatment (e.g., **Couvreur et al. 2012**; **Pointurier et al.**

226 2021), whereas ecosystem models often need to balance biological and ecological complexity with
227 computational efficiency. Further increasing complexity by having more pools to account for each
228 fine-root order would likely fall into the trap of diminishing returns in performance with an
229 increasing parameterization challenge (e.g., **Transtrum et al. 2015**).

230 Parameterization of a 3-pool TAM structure has empirical support across organizational
231 and spatial-temporal scales in the biosphere. TAM confers generality across scales by enabling
232 adaptable fine-root pools. While T and A capture widespread functional differentiation between
233 transport and absorption, they can be effectively reduced to one pool to accommodate rare species
234 without such a clear differentiation (**McCormack et al. 2015a**). Also, the M pool, in practice, can
235 be attributed to hyphal mycelium of arbuscular (AM), ectomycorrhizal (ECM), and/or ericoid
236 fungi, depending on the specific site and/or geographic context (e.g., **Read 1991; Soudzilovskaia**
237 **et al. 2015**). Besides this adaptability, the empirical support is facilitated by availability of trait
238 databases. In the context of a belowground data revolution [see a synthesis by **Iversen and**
239 **McCormack (2021)**], databases with increasing spatial coverage of explicit fine-root traits and
240 fungal traits aggregated from either function- or order-based measurement make it feasible to
241 parameterize TAM across scales in terrestrial ecosystem models. Notably, the Fine-Root Ecology
242 Database (FRED), houses root trait observations from across c. 4600 unique plant species and
243 continues to grow (**Iversen et al. 2017; Iversen and McCormack 2021**). Such an empirical
244 support warrants realizing and testing TAM in terrestrial ecosystem models.

245

246



247

248 **Fig. 2 Realizing TAM with a feasibility-realism tradeoff in terrestrial ecosystem models**
249 **under three paradigms of vegetation structure.** The landscape of vegetation, particularly
250 forests, is a mosaic of gaps (or patches) at different successional stages under exogenous and
251 endogenous disturbances, structuring vegetation dynamics both vertically and horizontally
252 by age (e.g., **Watt 1947; Bormann and Likens 1979**). The three paradigms capture such pattern
253 and process of vegetation to different extents. Big-leaf models (e.g., ELM), representing global
254 vegetation in fractional coverage using a few PFTs, do not capture local plant diversity and cannot
255 predict structural dynamics. By contrast, in capturing the vertical and spatial structure of forests,
256 individual-based forest gap models explicitly simulate growth, mortality, and reproduction of very
257 single individual in an array of gaps (e.g., **Shugart 1984; Shugart et al. 2018**). By approximating

258 the spatial and vertical structuring of vegetation without an explicit parameterization of different
259 individuals (e.g., **Kohyama 1993**), cohort-based models [e.g., FATES: Functionally Assembled
260 Terrestrial Ecosystem Simulator (**Fisher et al. 2018**) and ED: Ecosystem Demography model
261 (**Moorecroft et al. 2001**)] simplify individual-based gap models by utilizing cohorts of like-sized
262 plants under the traditional PFT scheme. Models under these paradigms assume a single fine-root
263 pool; realizing TAM in these models can capture different organizational levels across spatio-
264 temporal scales in the biosphere. ELM, as a representative of the relatively simplest big-leaf model,
265 is taken as an example for TAM demonstration in this viewpoint.

266

267 **3. Realizing the TAM structure in terrestrial ecosystem models**

268 To realize TAM in terrestrial ecosystem models, we propose a high-level framework of
269 partitioning, phenology, and distribution to encapsulate processes towards simulating a temporally
270 and vertically resolved 3-pool fine-root system (**Fig.1**). Partitioning is responsible for determining
271 the magnitude of carbon allocated from recent photosynthates or storage to the T, A, and M pools,
272 which is dynamic in nature arising from changes in biotic and abiotic environment from edaphic
273 factors (e.g., nutrient availability) to atmospheric changes (e.g., elevated CO₂) (**Mooney 1972**;
274 **Chapin et al. 2009; Drigo et al. 2010; Gorka et al. 2019; Ouimette et al. 2020; Prescott et al.**
275 **2020**). Phenology then controls the timing of partitioning. Here, we are highlighting phenology as
276 an essential component because of recurring observations of above- and below-ground
277 phenological asynchronicity (e.g., **Steinaker et al. 2010; Abramoff & Finzi 2015; McCormack**
278 **et al. 2015b; Radville et al. 2016; Iversen et al. 2018**). In addition to variations in phenology
279 among the TAM structures, phenology varies with soil depth (e.g., **Maeght et al. 2015**). This
280 vertical variability makes it essential to represent the vertical distribution within the soil profile of

281 carbon and nutrients partitioned to TAM pools at each time-step (e.g., **Tumber-Dávila et al.**
282 **2022**). Moreover, traits of fine roots and mycorrhizal fungi vary vertically (e.g., **McElrone et al.**
283 **2004; Robin et al. 2019**). This vertical variability feeds back to influence partitioning. Therefore,
284 these three components are interrelated in such a way that requires a close coupling of dynamic
285 partitioning with phenology temporally and distribution vertically. These components and their
286 interactions can be integrated into existing models by coupling with upstream photosynthesis and
287 allocation and with downstream soil biogeochemistry.

288 Starting this integration from a simple model structure is practical in the sense of observing
289 impacts of TAM while paving the way for realization and evaluation in more complicated model
290 structures (**Fig.2**). Existing models, built with different assumptions for different purposes, vary
291 in their structural realism of representing vegetation pattern and process under three different
292 paradigms. Integrating TAM into models under these paradigms can incorporate different
293 organizational levels across spatial-temporal scales, which, though exciting, trades off with
294 feasibility in terms of formulation, parameterization, and evaluation. Testing proof-of-concept
295 impacts of TAM under the relatively simple big-leaf paradigm is expected to help identify both
296 opportunities and challenges to realize TAM under structurally more realistic vegetation
297 paradigms.

298 Therefore, we examine impacts of TAM in the context of the state-of-the-art Energy
299 Exascale Earth System Model Land Model, ELM. ELM is a typical big-leaf model with a single
300 fine-root pool based on the traditional scheme of representing global plant diversity using
301 relatively few PFTs, which has been extensively used for land-atmosphere interactions regionally
302 and globally (e.g., **Golaz et al. 2019; Burrows et al. 2020**). Moreover, ELM uses the relative-
303 demand approach as a default configuration for plant-microbe nutrient competition (**Box 1**), which

304 does not require an explicit representation of fine-root and fungal functions and remains a
305 prevailing approach in earth system modelling as a simplification of plant-microbe competition
306 for nutrients (e.g., **Thornton et al. 2007; Yang et al. 2014**). Such formulations of ELM make it
307 feasible for building and testing the TAM structure for a proof-of-concept purpose.

Table 1 Measured traits used to parameterize TAM in the example realization and expected to be used to directly parameterize a functionally explicit TAM in terrestrial ecosystem models.

Category	Trait	T	A	M	Database
chemistry	stoichiometry				FRED
	chemical composition				FRED
demography	longevity				FRED
	phenology				
morphology	diameter				FRED
	tissue density				FRED
	specific root length				FRED
physiology/metabolism	respiration rate				FRED
	temperature sensitivity of respiration ($Q10$)				
	transporter enzyme production rate				
	exoenzyme production rate				
nutrient acquisition	transporter enzyme kinetics (Km & $Vmax$)				
	exoenzyme degradation kinetics (Km & $Vmax$)				
water uptake	hydraulic conductivity				FRED
	water uptake				
profile	max rooting depth				FRED, RSIP

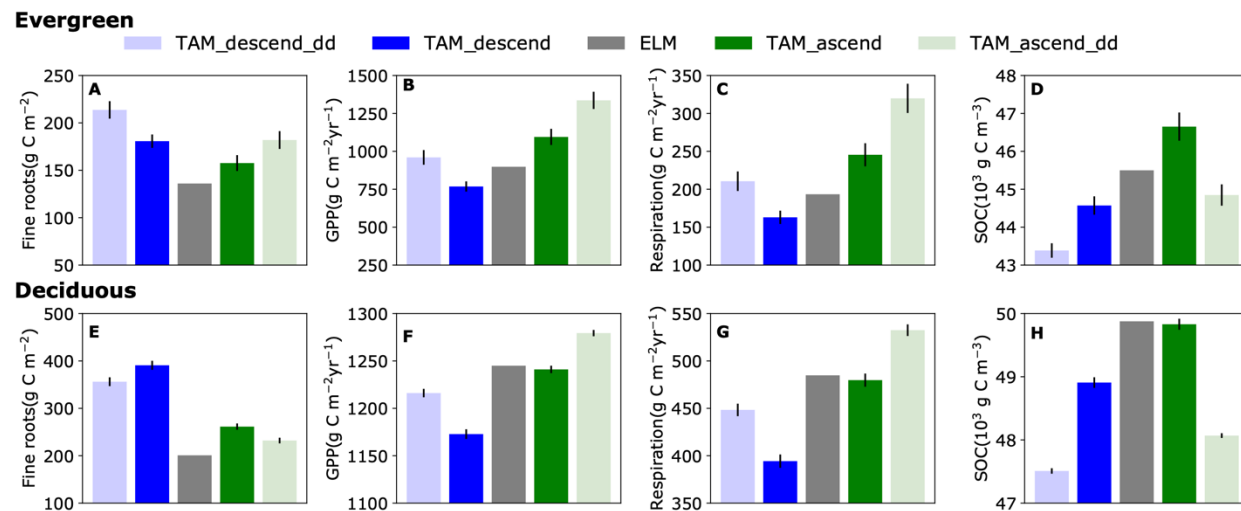
Note that the traits listed above are those that can directly inform TAM parameterization. Many of the measurements listed in databases (e.g., FRED) are emergent properties and could instead be used for model validation. Bolded traits are used for demonstration in this viewpoint, while grey cells indicate applicability of the traits to TAM. Database indicates coverage of the traits by FRED (which does not necessarily mean a full coverage of all TAM structures) or not (which clearly suggest targets of more empirical efforts). RSIP (Root Systems of Individual Plants) database is a primary source for root system size. See **Iversen and McCormack (2022)** for a synthesis of available databases of fine-root and mycorrhizal fungi traits.

309 **4. Impacts of TAM on forest ecosystems: an example realization**

310 We introduced a series of specific changes within the above framework to realize a 3-pool
311 TAM structure and examined its impacts against the 1-pool structure in ELM. In contrast to the
312 constraint of a single-pool structure, TAM allows trait divergence (**Box 1**) among the fine-root and
313 fungal pools with respect to carbon to nitrogen ratio (C/N), longevity, and chemical composition,
314 as well as respiration (**Table 1**), following observed trait variability within fine-root systems [see
315 the synthesis of **McCormack et al. (2015a)**]. To partition the carbon fixed by a plant to each of
316 the TAM pools, we introduced three parameters—fractions of the total allocation to a fine-root
317 system determined by the prevailing assumption of a 1:1 allometry between leaf and fine-root
318 system. These fractions together with C/N of the three TAM pools determine the C/N of bulk fine-
319 root system (**Eq. 1** in the **Appendix**), which, in combination with other structural tissues (leaf,
320 stem, and coarse-root), determine whole-plant stoichiometry and thus dictate nitrogen demand and
321 uptake under the demand-driven approach. We then decoupled the timing of partitioning to TAM
322 pools from leaf phenology, enabling an independent control on initiation (as a function of growing
323 degree days) and turnover (determined by prescribed longevity) of TAM for both deciduous and
324 evergreen PFTs. The turnover is further constrained by a depth-correction term to capture the
325 widely observed pattern of decreasing turnover with soil depth (e.g., **Baddeley and Waston 2005**;
326 **McCormack et al. 2012; Gu et al. 2017**). To vertically distribute the carbon partitioned to TAM
327 pools within the soil profile we introduced a formulation of dynamic distribution based on
328 changing profile of nutrient availability instead of the prevailing static assumption (e.g., **Zeng**
329 **2001; Drewniak 2019**). This nutrient-based dynamic distribution allows more of the partitioning
330 to go to the depth where the relative availability of nitrogen is higher. We implemented these
331 changes to different extents to examine structural uncertainty while accounting for parameter

332 uncertainty in a deciduous forest and an evergreen forest in the temperate forest biome of North
333 America only for an illustration of impacts of TAM against ELM (see **Methods** in the **Appendix**
334 for details).

335



336

337 **Fig. 3 TAM impacts against the 1-pool fine-root model on temperate evergreen (A-D) and**
338 **deciduous forests (E-H) under preservation of the bulk fine-root C/N.** The preservation is
339 differentiated between two partitioning patterns: TAM_descend (increasingly less partitioned to
340 mycorrhizal fungi) and TAM_ascend (increasingly more partitioned to the mycorrhizal fungi), on
341 top of which comparisons are made by further adding dynamic distribution (TAM_descend_dd
342 and TAM_ascend_dd). Note these comparisons were made under an assumption of the same
343 phenology between TAM and ELM. Fluxes of GPP (B, F) and heterotrophic respiration (C, G)
344 are aggregated annual values, while pools of fine-root mass and SOC are mean daily values. The
345 variance (95% confidence interval) arises from parameter uncertainty with respect to longevity
346 and fine-root chemistry. Note different y-axis scales across panels are for distinguishing between
347 different scenarios. See seasonal dynamics of GPP and fine roots, as well as leaf biomass in
348 **Supplementary Fig. 1** in the **Appendix**.

349 **4.1 TAM impacts under preservation of bulk fine-root stoichiometry**

350 First, changing the structure from 1 to 3 pools but preserving the C/N of bulk fine-root
351 system can give us a parsimonious view of impacts arising from trait divergence in TAM. A direct
352 reason of preservation (**Box 1**) is that C/N of the bulk fine-root system, in principle, should be the
353 same irrespective of the number of pools used in model representation. Keeping the same C/N is
354 also useful in the sense of using existing field observations of bulk fine-root C/N to constrain the
355 model. More importantly, with a demand-driven approach in ELM, C/N of the bulk fine-root
356 system instead of C/N of any of the TAM components dictates plant nitrogen demand and uptake.
357 Therefore, a preservation provides two benefits: it keeps the same nutrient uptake capability as the
358 single-pool model while capturing the divergence in C/N among TAM pools. The preservation is
359 achieved via pairing a set of C/N values with a set of partitioning fractions of TAM (see **Methods**
360 in the **Appendix**). To capture the wide spectrum of plant partitioning variability among different
361 belowground sinks, we consider two sets of partitioning fractions forming two contrasting
362 partitioning patterns: a descending pattern (i.e., increasingly less carbon partitioned to the
363 mycorrhizal fungi) and an ascending pattern (i.e., increasingly more carbon partitioned to the
364 mycorrhizal fungi). Under both patterns, the tissue C/N decreases while turnover increases from
365 T, to A, and then to the M pool; the M has the lowest C/N and fastest turnover, reflecting their
366 consistently lower C/N and short lifespans (**Allen and Kitajima 2013; Zanne et al. 2020**). Under
367 the same phenology, we compared TAM under the two partitioning patterns against ELM first by
368 assuming the same fixed vertical distribution and then by adding dynamic vertical distribution
369 contingent on relative nutrient availability (**Fig. 3**).

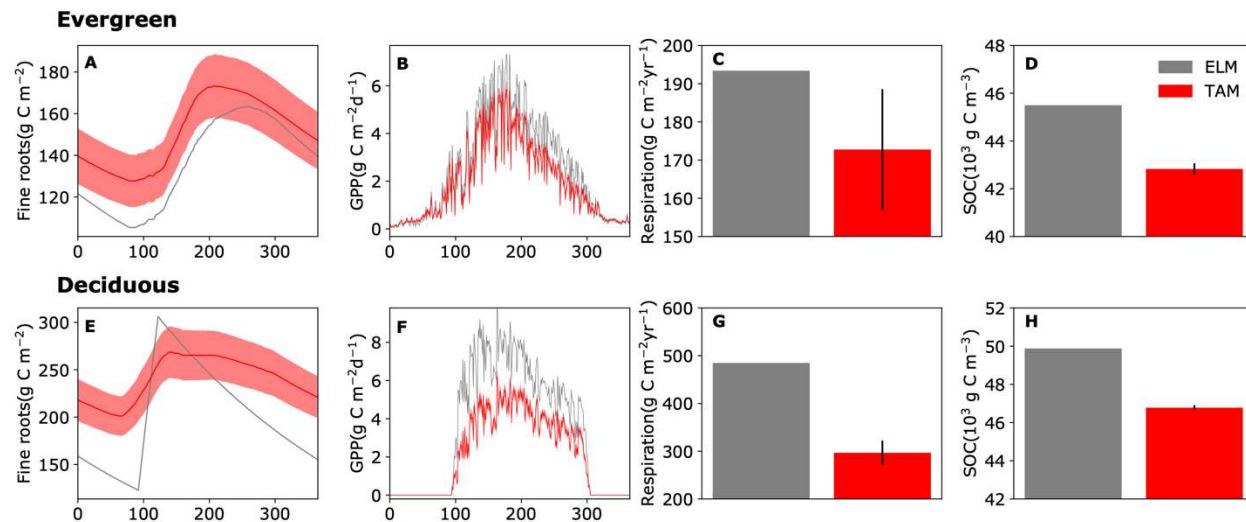
370 With the same static distribution, since both the stoichiometry and the phenology are the
371 same, significant partitioning-dependent impacts of TAM compared against the 1-pool model can

372 be attributed to changes in turnover and litter inputs arising from explicit low to high turnover rates
373 and high to low C/N moving from T through M pools. The impacts are directly reflected in changes
374 in fine-root biomass (including mycorrhizal hyphae biomass). When reaching equilibrium in both
375 the evergreen and deciduous forest, under the descending partitioning pattern total fine-root
376 biomass increased relative to the single-pool model owing to the lowest turnover rate of T roots
377 (**Fig. 3A, E**). Similar, but somewhat dampened responses, were seen under the ascending pattern
378 as there was relatively more carbon portioned to the M pool which has the highest turnover rate
379 and resulted in less total standing biomass. These changes under equilibrium also came from
380 feedbacks associated with changing temporal patterns of fine-root litter inputs and subsequent
381 changes in GPP (**Fig. 3B, F**), soil heterotrophic respiration (**Fig. 3C, G**), and soil organic carbon
382 storage (**Fig. 3D, H**), although these shifts were insignificant for the deciduous forest under the
383 ascending pattern.

384 Enabling the dynamic vertical distribution further enhanced the effects of changing
385 turnover of fine-root systems and hence litter inputs according to soil nutrient availability. Because
386 this dynamic distribution increased inputs of fine-root and mycorrhizal fungal litters into soil layers
387 where N availability was relatively higher, a reduction in N limitation led to increased soil
388 respiration and GPP (**Fig. 3D, H**) but with a net effect of soil carbon stock decline under both
389 patterns (**Fig. 3C, G**). However, fine-root biomass experienced a continued increase in the
390 evergreen forest compared to a pause in the deciduous forest because relatively more biomasses
391 accumulated in deeper soils with slower turnover rates in evergreen forest than in the deciduous
392 forest (**Fig. 3D, H**). These new changes under dynamic distribution highlight the role of vertical
393 variability of TAM in influencing plant-soil interactions. In short, even parsimonious TAM has

394 important implications for carbon cycling under stoichiometry preservation while capturing
395 observed differentiation within fine-root systems.

396



397 **Fig. 4 TAM impacts against the 1-pool fine-root model on temperate evergreen (A-D) and**
398 **deciduous forests (E-H) without the restraint of preservation.** Respiration is aggregated annual
399 values (C, G) and SOC is averaged across a whole year (D, H). The variance (95% confidence
400 interval) arose from accounting for all uncertain parameters introduced to realize TAM (see
401 interval) arose from accounting for all uncertain parameters introduced to realize TAM (see
402 **Supplementary Table 1**).

403

404 **4.2 TAM dampens forest productivity and soil carbon storage**

405 Implementing TAM without the constraint of stoichiometry preservation consistently
406 resulted in reduced ecosystem productivity and soil carbon stock regardless of forest type
407 compared to the 1-pool model (Fig. 4). With a full accounting of parameter uncertainty informed
408 by observations (see **Methods** in **Appendix** for details), on average annual GPP was reduced by
409 20.3 % and 36.3 % while soil organic carbon was reduced by 5.9 % and 6.2 % in the evergreen
410 and deciduous forests, respectively. These reductions in equilibrium originated from changing

411 allocation (different C/N of fine-root systems) and explicit fine-root turnover, as indicated by the
412 increased, though not seasonally consistent, fine-root biomass in equilibrium (**Fig. 4A, E**). Over
413 time these changes led to aggravated nutrient limitation (**Supplementary Fig. 2**), together with
414 decreased leaf area, contributing to declines in GPP (**Fig. 4B, F**). Such a GPP reduction eventually
415 resulted in decreased heterotrophic respiration and a net decline of soil organic carbon (**Fig. 4D,**
416 **H**). These robust changes arising from TAM suggest that 1-pool models may overestimate forest
417 productivity and soil carbon storage, which is in line with the general notion of a lack of accurate
418 sink-limited growth in current terrestrial ecosystem models leading to an overestimation of land
419 carbon sink (e.g., **Cabon et al. 2022**). In summary, the improved realism of TAM informed by
420 empirical trait divergence can show robust impacts while accounting for parameter uncertainty.

421

422 **4.3 TAM echoes embracing complexity in ecosystem modelling in general**

423 These results provide strong quantitative support for TAM. The examples above
424 demonstrate significant impacts of the explicit TAM structure against a homogeneous single-pool
425 structure while accounting for structural and parameter uncertainty, especially considering the case
426 of parsimonious stoichiometry preservation. Admittedly, this demonstration is based on only one
427 simplified, though generally representative, vegetation modelling scheme, and it remains
428 premature to claim that this TAM structure has improved model predictability without testing
429 TAM across a broader range of sites in demography models (**Fig. 2**). However, such a shift from
430 implicit to explicit reflects a broad notion of embracing biological and ecological complexity in
431 ecosystems from above- to below-ground to improve model performance. A notable aboveground
432 shift in vegetation structure is from the big-leaf approach using a single-layer canopy to explicitly
433 modeling multi-layer canopy structures (e.g., **Sinclair et al., 1976; Norman, 1993; Yan et al.**

434 **2017; Bonan et al. 2021**), and further to a paradigm simulating vegetation dynamics in the spatial
435 and vertical structuring by age and size (e.g., **Shugart 1984; Kohyama 1993; Moorcroft et al.**
436 **2001; Wang et al. 2016; Shugart et al. 2018; Fisher et al. 2018**). A similar belowground example
437 is the shift from simulating the tremendously complex soil microbiomes first implicitly (e.g.,
438 **Parton et al. 1987**), then as a ‘big microbe (e.g., **Allison et al. 2010**), and more recently as a
439 constellation of a few discrete functional groups (e.g., **Wieder et al. 2015**) or even of continuous
440 hypothetical individuals using a trait-based approach (**Wang and Allison 2022**) in a structurally
441 explicit soil environment (**Wang et al. 2019**). Echoing this trend of effectively embracing
442 ecological complexity, we present empirical and theoretical bases for the TAM structure and
443 demonstrate its impacts, arguably suggesting a move beyond the single fine-root pool paradigm in
444 terrestrial ecosystem modelling, which, however, still needs to confront a myriad of uncertainties
445 and challenges.

446

447 **5. Uncertainties and challenges in realizing the TAM structure**

448 Lingering uncertainties and challenges are closely tied to prevailing model assumptions as
449 exemplified in the example realization. First, parameter uncertainties point us to a challenge of
450 constraining partitioning while improving the representations of phenology and distribution in
451 general. Second, going beyond the simplistic demand-driven nutrient acquisition assumption to
452 integrate fine-root and mycorrhizal fungal functions with TAM will necessitate significant
453 theoretical explorations and empirical investigations for model formulation, parameterization, and
454 validation. However, to eventually realize TAM in ecologically realistic demography models
455 (**Fig.2**), new challenges will emerge regarding age- and size-based changes in TAM that the big-
456 leaf paradigm neglects, especially in ecosystems of high biological diversity.

457

458 **5.1 A unified framework to simulate partitioning, phenology, and distribution**

459 Partitioning, a key component in realizing a 3-pool TAM structure, is the most outstanding
460 uncertainty. Sensitivity analyses (see **Methods in the Appendix**) show the parameters controlling
461 partitioning are among the most sensitive ones (**Supplementary Fig. 3**). A direct reason for this
462 sensitivity to partitioning is trait divergence from 1 to 3 pools with respect to, e.g., C/N, longevity,
463 and chemical composition, as well as vertical differentiation in turnover time (**Table 1**). In addition
464 to more constrained parameterizations of these traits, more accurate partitioning is essential for
465 uncertainty reduction. Constraining the uncertainty of partitioning, however, is not as
466 straightforward as simply improving parameterization of TAM traits, which can be informed by
467 more field measurements. Instead, the interactive nature among partitioning, phenology, and
468 vertical distribution, as indicated in **Section 3**, calls for a unified framework to simulate dynamic
469 partitioning while accurately treating phenology and distribution to reduce the associated
470 uncertainties.

471 Optimization techniques may offer such a unified framework, but it still faces a few
472 immediate challenges. First, finding appropriate objectives for optimization with a balanced
473 perspective of both plant and mycorrhizal fungi is non-trivial (e.g., **Bloom et al. 1985; Koide and**
474 **Elliot 1989**). In addition, understanding of both phenology and distribution of TAM are in their
475 infancy. Phenology is influenced by a plethora of factors including endogenous cues (**Joslin et al.**
476 **2001; Tierney et al. 2003**) and exogenous, abiotic cues (e.g., **Radville et al. 2016**), as well as
477 microbial processes in the soil [see the review by **O'Brien et al. (2021)**]. This complex regulation
478 is evident from mounting observations of variability in numbers of fine-root growth peaks (e.g.,
479 **Steinaker et al. 2010; McCormack et al. 2015b**) and of complex life history strategies of

480 mycorrhizal fungi with spore dormancy (e.g., **Gianinazzi-Pearson et al., 1989; Bago et al. 2000;**
481 **Defrenne et al. 2021**). TAM variability in phenology is far from being robust as it cannot yet
482 account for all relevant abiotic factors. However, an independent treatment of TAM initiation and
483 mortality allowing for asynchronous phenology between leaves and fine-root systems represents a
484 substantial improvement. Still, the lack of asynchronous TAM phenology vertically means that the
485 timing of partitioning at each depth is not fully accurate. Also, dynamic distribution, though
486 constrained by dynamic nutrient availability in the soil profile, needs to account for other important
487 factors (e.g., soil moisture and temperature). Addressing these interrelated processes under an
488 optimization framework requires not only explicit seasonal observations of fine-root system
489 dynamics across root orders and mycorrhizal fungi within soil profiles to disentangle
490 environmental controls but requires explicit TAM functioning that goes beyond the demand-driven
491 approach.

492

493 **5.2 Connecting TAM with fine-root and mycorrhizal fungal functions**

494 Relaxing the assumption of demand-driven nutrient uptake and competition entails an
495 explicit formulation of the different functions of T, A and M pools and their interactions with soils.
496 Incorporating explicit TAM functioning with respect to nutrient and water uptake will require
497 explicit absorptive root and mycorrhizal fungi traits (**Table 1**) related to uptake of nutrients in
498 various forms of nitrogen and phosphorous (e.g., **Yang et al. 2014; 2019**) and water (e.g.,
499 **Polverigiani et al. 2011; Jackisch et al. 2020; Kakouridis et al. 2020; Mackay et al. 2020**).
500 Notably, mycorrhizal fungi in TAM, especially ectomycorrhiza and ericoid mycorrhiza, can
501 directly mediate litter and soil organic matter decomposition by exuding enzymes and taking up
502 organic nitrogen (e.g., **Gadgil and Gadgil 1971; Frey 2019**). Therefore, once TAM incorporates

503 explicit root and mycorrhizal functions, it becomes highly necessary to make a concomitant change
504 to microbially-explicit organic matter decomposition with exoenzymes instead of the first-order
505 decomposition assumed in ELM. A microbially explicit decomposition model then needs to
506 accommodate fine-root system exudates while handling explicit litter decomposition arising from
507 the explicit turnover of TAM components, especially with fungal necromass (e.g., **Matamala et**
508 **al. 2003; Strand et al. 2008; Fernandez et al. 2013; Sun et al. 2018**). These aspects can be
509 addressed by combining a microbially explicit organic matter decomposition model interacting
510 with the functioning of fine-root systems (e.g., **Sulman et al. 2018; Wang and Allison 2019**) with
511 the existing approach of resolving plant-microbe competition for nutrient uptake based on the
512 Equilibrium Chemistry Approximation theory (**Zhu et al. 2017; Wang and Allison 2019**).
513 However, to capture the variability in these processes and their interactions arising from biological
514 diversity, we need to move beyond the big-leaf paradigm.

515

516 **5.3 Realizing TAM in demography models**

517 Moving forward from the big-leaf structure to realizing TAM in demography models will
518 require creative efforts to best capture patterns and processes belowground. The mosaic of forested
519 landscapes so far has only been emphasized aboveground, and while previous studies have
520 documented high heterogeneity in belowground processes, our example realization of TAM using
521 the big-leaf approach circumvents this challenge (**Fig.2**). One outstanding issue towards this end
522 is to simulate age- and size-related changes in TAM in the context of complete life cycles of
523 growth, mortality, and reproduction for many different individuals under disturbances. For
524 instance, evidence has indicated roles of mycorrhizal fungi change with plant community
525 succession stage (e.g., **Pankow et al. 1991; Read 1991; Nara 2006**). One strategy of simulating

526 age- and size-related changes would be conditioning TAM on a dynamic rooting depth of coarse
527 roots (constrained by, for example, maximum rooting depth; **Fig.1; Table 1**), instead of using a
528 constant value as widely assumed in current models. This change in rooting depth should involve
529 geometric and allometric relationships with aboveground structural tissues (e.g., **Eshel and**
530 **Grünzweig 2013; Brum et al. 2019; Tumber-Dávila et al. 2022**) while accounting for direct
531 influences from, for example, soil hydrological conditions (e.g., **Stone and Kalisz 1991; Fan et**
532 **al. 2007**). Addressing these aspects requires long-term observations of successional dynamics of
533 not only the aboveground but also the belowground (e.g., **Rees et al. 2001**; “**We must get a grip**
534 **on forest science — before it’s too late**”, **2022**).

535

536 **6. Implications of TAM for root ecology, ecosystem functioning, and ESMs**

537 Confronting those above challenges holds promise to stimulate empirical ecology of fine-
538 root systems, to drive theory-driven explorations of hypotheses of fine-root systems’ roles in
539 ecosystem functioning, and to improve the prognostic capability of ESMs. First, adopting this
540 structure would stimulate more targeted efforts at an increasing resolution of empirical research of
541 fine roots and mycorrhizal fungi as discussed above on challenges (**Table 1**). The proposal of
542 TAM is largely fueled by the belowground trait data revolution, especially with tremendous
543 empirical progress in collecting function- and/or order-based fine-root traits including microbial
544 associations (e.g., **McCormack et al. 2017; Iversen 2017; Iversen and McCormack 2017;**
545 **Freschet et al. 2021; Tedersoo et al. 2021**). Building on standardized measurement protocols
546 (**Freschet et al. 2021**), TAM may also stimulate further technical research and possible advances
547 in, for example, neutron imaging (e.g., **Warren et al. 2013**), remote sensing (e.g., **Sousa et al.**

548 2021), and machine learning in image recognition (e.g., **Han et al. 2021**), to speed up
549 characterization and classification of functional ‘roots’ within fine-root systems.

550 Undoubtedly, new measurements and causal relationships revealed by empiricists will
551 improve formulation, parameterization, and validation of TAM in models of increasing complexity
552 (**Fig. 2**). It is noteworthy that one of the major motivations for demography models is that local
553 community-level processes are essential in modelling ecosystem functioning responding to various
554 disturbances (e.g., **Wang et al. 2016; Fisher et al. 2018**). Increasing empirical and theoretical
555 studies have indicated that root competition may even be more important than aboveground
556 competition in shaping a plant community (e.g., **Gersani et al. 2001; Ljubotina and Cahill 2019;**
557 **Cabal et al. 2020; Sauter et al. 2021**). With this explicit structure of fine-root systems in
558 demography models of varying complexity, we can conduct theory-driven modelling studies to
559 explore hypotheses of root-associated community-level processes underlying ecosystem
560 functioning, which is otherwise challenging to experimentally track in the field.

561 We anticipate that all these empirical and theoretical advances arising from TAM
562 eventually will contribute to improving ESMs both directly and indirectly. A more accurate and
563 effective representation of fine-root systems across ecosystems may be directly incorporated into
564 terrestrial ecosystem models with different vegetation structures, as implied by the example
565 realization in temperate forest systems. Indirect benefits accompanying root improvement would
566 also likely follow by helping to identify sources of uncertainty in components of aboveground and
567 soil processes. One fundamental aspect might be to stimulate efforts to improve the scheme of
568 global plant functional type classification by systematically integrating belowground traits (e.g.,
569 **Smith et al. 1997; Phillips et al. 2013**). This indirect avenue is particularly promising considering
570 the historical dominance of top-down thinking in ESMs development (e.g., **Sellers et al. 1986**).

571 These direct and indirect effects together will improve the prognostic capability of ESMs to
572 evaluate biosphere-atmosphere interactions in the Earth system.

573

574 **7. Conclusions**

575 Uncertain terrestrial ecosystem models still contain a huge data-model discrepancy with
576 respect to fine-root system complexity. We speculate that closing this model-data gap will improve
577 the prognostic capability of models across scales. To effectively simulate this complexity, we
578 propose a function-based, 3-pool TAM structure representing transport and absorptive fine roots
579 and mycorrhizal fungi to approximate the high-dimensional structural and functional variations
580 within fine-root systems. Building upon theoretical and empirical bases of TAM as a balanced
581 approximation between realism and simplicity, we quantitatively confirmed the significance of
582 TAM for pools and fluxes of temperate forests arising from capturing the structural and functional
583 differentiation within fine-root systems in a big-leaf land surface model. Though uncertainties and
584 challenges remain towards realizing TAM in explicit demography models, TAM opens the door
585 for more realistically and effectively capturing fine-root systems complexity underlying their
586 functioning to eventually contribute to uncertainty reduction in ESMs.

587

588 **Acknowledgements**

589 The Fine-Root Ecology Database (FRED), BW, CMI, DR, and XY were supported by the
590 Biological and Environmental Research program within the Department of Energy's Office of
591 Science. The code of simple_ELM in Python is accessible at
592 https://github.com/dmricciuto/simple_ELM/tree/rootcomplexity. Outputs from the simulations
593 and code of analysis and visualization in Python are available at

594 <https://github.com/bioatmosphere/TAM>. This research used resources of the Compute and Data
595 Environment for Science (CADES) at the Oak Ridge National Laboratory, which is supported by
596 the Office of Science of the U.S. Department of Energy under Contract No. DE-AC05-
597 00OR22725.

598

599 **Author Contributions**

600 BW, MLM, DMR, XY, and CMI designed the research. BW performed the research, analyzed
601 data, and wrote the first manuscript draft. MLM, DMR, XY, and CMI contributed to results
602 interpretation and manuscript editing.

603

604 **Data Availability**

605 The code of simple_ELM in Python is accessible at
606 https://github.com/dmricciuto/simple_ELM/tree/rootcomplexity. Outputs from the simulations
607 and code of analysis and visualization in Python are available at
608 <https://github.com/bioatmosphere/TAM>. The database FRED is accessible at
609 <https://roots.ornl.gov/>.

610

611 **References**

612 Abramoff, R. Z., & Finzi, A. C. (2015). Are above-and below-ground phenology in sync? New
613 Phytologist, 205, 1054-1061.

614

615 Allen, M. F., & Kitajima, K. (2013). In situ high-frequency observations of mycorrhizas. New
616 Phytologist, 200, 222-228.

617

618 Allison, S. D., Wallenstein, M. D., & Bradford, M. A. (2010). Soil-carbon response to warming
619 dependent on microbial physiology. *Nature Geoscience*, 3, 336-340.

620

621 Atucha, A., Workmaster, B. A., & Bolivar-Medina, J. L. (2021). Root growth phenology, anatomy,
622 and morphology among root orders in *Vaccinium macrocarpon* Ait. *Botany*, 99, 209-219.

623

624 Baddeley, J. A., & Watson, C. A. (2005). Influences of root diameter, tree age, soil depth and
625 season on fine root survivorship in *Prunus avium*. *Plant and Soil*, 276, 15-22.

626

627 Bago, B., Pfeffer, P. E., & Shachar-Hill, Y. (2000). Carbon metabolism and transport in arbuscular
628 mycorrhizas. *Plant Physiology*, 124, 949-958.

629

630 Bardgett, R. D., Mommer, L., & De Vries, F. T. (2014). Going underground: root traits as drivers
631 of ecosystem processes. *Trends in Ecology & Evolution*, 29, 692-699.

632

633 Bloom, A. J., Chapin, F. S., & Mooney, H. A. (1985). Resource limitation in plants--an economic
634 analogy. *Annual review of Ecology and Systematics*, 363-392.

635

636 Bormann, F. H., & Likens, G. E. (1979). Catastrophic disturbance and the steady state in northern
637 hardwood forests: A new look at the role of disturbance in the development of forest ecosystems
638 suggests important implications for land-use policies. *American Scientist*, 67, 660-669.

639

640 Bonan, G. B., Patton, E. G., Finnigan, J. J., Baldocchi, D. D., & Harman, I. N. (2021). Moving
641 beyond the incorrect but useful paradigm: reevaluating big-leaf and multilayer plant canopies to
642 model biosphere-atmosphere fluxes—a review. *Agricultural and Forest Meteorology*, 306, 108435.

643

644 Bonan, G. B., & Doney, S. C. (2018). Climate, ecosystems, and planetary futures: The challenge
645 to predict life in Earth system models. *SCIENCE*, 359(6375).

646

647 Brum, M., Vadeboncoeur, M. A., Ivanov, V., Asbjornsen, H., Saleska, S., Alves, L. F., ... &
648 Oliveira, R. S. (2019). Hydrological niche segregation defines forest structure and drought
649 tolerance strategies in a seasonal Amazon forest. *Journal of Ecology*, 107, 318-333.

650

651 Brzostek, E. R., J. B. Fisher, and R. P. Phillips (2014), Modeling the carbon cost of plant nitrogen
652 acquisition: Mycorrhizal trade-offs and multipath resistance uptake improve predictions of
653 retranslocation. *J. Geophys. Res. Biogeosci.*, 119, 1684–1697

654

655 Burrows, S. M., Maltrud, M., Yang, X., Zhu, Q., Jeffery, N., Shi, X., ... & Leung, L. R. (2020).
656 The DOE E3SM v1.1 biogeochemistry configuration: Description and simulated ecosystem-
657 climate responses to historical changes in forcing. *Journal of Advances in Modeling Earth
658 Systems*, 12, e2019MS001766.

659

660 Cabal, C., Martínez-García, R., de Castro Aguilar, A., Valladares, F., & Pacala, S. W. (2020). The
661 exploitative segregation of plant roots. *Science*, 370, 1197-1199.

662

663 Cabon, A., Kannenberg, S. A., Arain, A., Babst, F., Baldocchi, D., Belmecheri, S., ... & Anderegg,
664 W. R. (2022). Cross-biome synthesis of source versus sink limits to tree growth. *Science*, 376,
665 758-761.

666

667 Defrenne, C. E., Childs, J., Fernandez, C. W., Taggart, M., Nettles, W. R., Allen, M. F., ... &
668 Iversen, C. M. (2021). High-resolution minirhizotrons advance our understanding of root-fungal
669 dynamics in an experimentally warmed peatland. *Plants, People, Planet*, 3, 640-652.

670

671 Chapin III, S. F., McFarland, J., David McGuire, A., Euskirchen, E. S., Ruess, R. W., & Kielland,
672 K. (2009). The changing global carbon cycle: linking plant–soil carbon dynamics to global
673 consequences. *Journal of Ecology*, 97, 840-850.

674

675 Couvreur, V., Vanderborght, J., & Javaux, M. (2012). A simple three-dimensional macroscopic
676 root water uptake model based on the hydraulic architecture approach. *Hydrology and Earth
677 System Sciences*, 16, 2957-2971.

678

679 Drewniak, B. A. (2019). Simulating dynamic roots in the energy exascale earth system land model.
680 *Journal of Advances in Modeling Earth Systems*, 11, 338-359.

681

682 Drigo, B., Pijl, A. S., Duyts, H., Kielak, A. M., Gamper, H. A., Houtekamer, M. J., ... &
683 Kowalchuk, G. A. (2010). Shifting carbon flow from roots into associated microbial communities
684 in response to elevated atmospheric CO₂. *Proceedings of the National Academy of Sciences*, 107,
685 10938-10942.

686

687 Eshel, A., & Grünzweig, J. M. (2013). Root–shoot allometry of tropical forest trees determined in
688 a large-scale aeroponic system. *Annals of botany*, 112, 291-296.

689

690 Fan, Y., Miguez-Macho, G., Jobbágy, E. G., Jackson, R. B., & Otero-Casal, C. (2017). Hydrologic
691 regulation of plant rooting depth. *Proceedings of the National Academy of Sciences*, 114, 10572-
692 10577.

693

694 Fernandez, C. W., & Kennedy, P. G. (2018). Melanization of mycorrhizal fungal necromass
695 structures microbial decomposer communities. *Journal of Ecology*, 106, 468-479.

696

697 Fisher, R. A., Koven, C. D., Anderegg, W. R., Christoffersen, B. O., Dietze, M. C., Farrior, C. E.,
698 ... & Moorcroft, P. R. (2018). Vegetation demographics in Earth System Models: A review of
699 progress and priorities. *Global Change Biology*, 24, 35-54.

700

701 Fitter, A. H. (1982). Morphometric analysis of root systems: application of the technique and
702 influence of soil fertility on root system development in two herbaceous species. *Plant, Cell &*
703 *Environment*, 5, 313-322.

704

705 Frey, S. D. (2019). Mycorrhizal fungi as mediators of soil organic matter dynamics. *Annual
706 Review of Ecology, Evolution, and Systematics*, 50(1).

707

708 Friend, A. D., Lucht, W., Rademacher, T. T., Keribin, R., Betts, R., Cadule, P., ... & Woodward,
709 F. I. (2014). Carbon residence time dominates uncertainty in terrestrial vegetation responses to
710 future climate and atmospheric CO₂. *Proceedings of the National Academy of Sciences*, 111, 3280-
711 3285.

712

713 Gadgil, R., Gadgil, P. (1971). Mycorrhiza and Litter Decomposition. *Nature* **233**, 133.

714 <https://doi.org/10.1038/233133a0>

715

716 Gersani, M., Brown, J. S., O'Brien, E. E., Maina, G. M., & Abramsky, Z. (2001). Tragedy of the
717 commons as a result of root competition. *Journal of Ecology*, 89, 660-669.

718

719 Gianinazzi-Pearson, V., B. Branzanti, and S. Gianinazzi. 1989. In vitro enhancement of spore
720 germination and early hyphal growth of a vesicular-arbuscular mycorrhizal fungus by host root
721 exudates and plant flavonoids. *Symbiosis* 7, 243–255.

722

723 Gorka, S., Dietrich, M., Mayerhofer, W., Gabriel, R., Wiesenbauer, J., Martin, V., ... & Kaiser, C.
724 (2019). Rapid transfer of plant photosynthates to soil bacteria via ectomycorrhizal hyphae and its
725 interaction with nitrogen availability. *Frontiers in Microbiology*, 10, 168.

726

727 Grime, J. P. (1974). Vegetation classification by reference to strategies. *Nature* 250, 26–31.

728

729 Guo, D., Xia, M., Wei, X., Chang, W., Liu, Y., & Wang, Z. (2008). Anatomical traits associated
730 with absorption and mycorrhizal colonization are linked to root branch order in twenty-three
731 Chinese temperate tree species. *New Phytologist*, 180, 673-683.

732

733 Han, Eusun, Abraham George Smith, Roman Kemper, Rosemary White, John A Kirkegaard,
734 Kristian Thorup-Kristensen, Miriam Athmann. (2021). Digging roots is easier with AI. *Journal of*
735 *Experimental Botany*, 13, 4680–4690

736

737 Hishi, T., & Takeda, H. (2005). Dynamics of heterorhizic root systems: protoxylem groups within
738 the fine-root system of *Chamaecyparis obtusa*. *New Phytologist*, 167, 509-521.

739 Hunt, H. W., Trlica, M. J., Redente, E. F., Moore, J. C., Detling, J. K., Kittel, T. G. F., ... & Elliott,
740 E. T. (1991). Simulation model for the effects of climate change on temperate grassland
741 ecosystems. *Ecological Modelling*, 53, 205-246.

742

743 Iversen, C. M. et al. (2017). A global Fine-Root Ecology Database to address below-ground
744 challenges in plant ecology. *New Phytologist*, 215, 15–26.

745

746 Iversen, C.M., Childs, J., Norby, R.J. et al. (2018). Fine-root growth in a forested bog is seasonally
747 dynamic, but shallowly distributed in nutrient-poor peat. *Plant and Soil* 424, 123–143.

748

749 Iversen, C. M., & McCormack, M. L. (2021). Filling gaps in our understanding of belowground
750 plant traits across the world: an introduction to a Virtual Issue. *New Phytologist*, 231, 2097-2103.

751

752 Jackisch, C., Knoblauch, S., Blume, T., Zehe, E., & Hassler, S. K. (2020). Estimates of tree root
753 water uptake from soil moisture profile dynamics. *Biogeosciences*, 17, 5787-5808.

754

755 Joslin, J. D., Gaudinski, J. B., Torn, M. S., Riley, W. J., & Hanson, P. J. (2006). Fine-root turnover
756 patterns and their relationship to root diameter and soil depth in a ¹⁴C-labeled hardwood forest.
757 *New Phytologist*, 172, 523-535.

758

759 Kakouridis, A., Hagen, J. A., Kan, M. P., Mambelli, S., Feldman, L. J., Herman, D. J., ... &
760 Firestone, M. K. (2020). Routes to roots: direct evidence of water transport by arbuscular
761 mycorrhizal fungi to host plants. <https://doi.org/10.1111/nph.1828>

762

763 Koide, R. & Elliot, G. (1989). Cost, benefit, and efficiency of the vesicular-arbuscular mycorrhizal
764 symbiosis. *Functional Ecology* 3, 252-255.

765

766 Kenrick, P., & Strullu-Derrien, C. (2014). The origin and early evolution of roots. *Plant
767 Physiology*, 166, 570-580.

768

769 King, W.L., Yates, C.F., Guo, J. et al. (2021). The hierarchy of root branching order determines
770 bacterial composition, microbial carrying capacity and microbial filtering. *Communication
771 Biology* 4, 483.

772

773 Kirschbaum, M. U., & Paul, K. I. (2002). Modelling C and N dynamics in forest soils with a
774 modified version of the CENTURY model. *Soil Biology and Biochemistry*, 34, 341-354.

775

776 Kleidon, A., & Heimann, M. (1998). Optimised rooting depth and its impacts on the simulated
777 climate of an atmospheric general circulation model. *Geophysical research letters*, 25, 345-348.

778

779 Klimešová, J., & Herben, T. (2021). The hidden half of the fine root differentiation in herbs:
780 nonacquisitive belowground organs determine fine-root traits. *Oikos*. doi: 10.1111/oik.08794

781

782 Kohyama, T. (1993). Size-structured tree populations in gap-dynamic forest--the forest
783 architecture hypothesis for the stable coexistence of species. *Journal of Ecology*, 81, 131-143.

784

785 Ljubotina MK, Cahill Jr JF. 2019 Effects of neighbour location and nutrient distributions on root
786 foraging behaviour of the common sunflower. *Proc. R. Soc. B* 286: 20190955.

787

788 Lovenduski, N. S., & Bonan, G. B. (2017). Reducing uncertainty in projections of terrestrial
789 carbon uptake. *Environmental Research Letters*, 12, 044020.

790

791 Mackay, D. S., Savoy, P. R., Grossiord, C., Tai, X., Pleban, J. R., Wang, D. R., ... & Sperry, J. S.
792 (2020). Conifers depend on established roots during drought: results from a coupled model of
793 carbon allocation and hydraulics. *New Phytologist*, 225, 679-692.

794

795 Maeght, J. L., Gonkhamdee, S., Clement, C., Isarangkool Na Ayutthaya, S., Stokes, A., & Pierret,
796 A. (2015). Seasonal patterns of fine root production and turnover in a mature rubber tree (*Hevea*

797 *brasiliensis* Müll. Arg.) stand-differentiation with soil depth and implications for soil carbon
798 stocks. *Frontiers in Plant Science*, 6, 1022.

799

800 Matamala, R., Gonzalez-Meler, M. A., Jastrow, J. D., Norby, R. J., & Schlesinger, W. H. (2003).
801 Impacts of fine root turnover on forest NPP and soil C sequestration potential. *Science*, 302, 1385-
802 1387.

803

804 McCormack, M.L., Adams, T. S., Smithwick, E. A., & Eissenstat, D. M. (2012). Predicting fine
805 root lifespan from plant functional traits in temperate trees. *New Phytologist*, 195, 823-831.

806

807 McCormack, M. L., I. A. Dickie, D. M. Eissenstat, T. J. Fahey, C. W. Fernandez, D. Guo, H.-S.
808 Helmisaari, E. A. Hobbie, C. M. Iversen, R. B. Jackson, J. Leppälämmi-Kujansuu, R. J. Norby, R.
809 P. Phillips, K. S. Pregitzer, S. G. Pritchard, B. Rewald, M. Zadworny (2015a). Redefining fine
810 roots improves understanding of below-ground contributions to terrestrial biosphere processes.
811 *New Phytologist*. 207, 505–518.

812

813 McCormack, M. L., Gaines, K. P., Pastore, M., & Eissenstat, D. M. (2015b). Early season root
814 production in relation to leaf production among six diverse temperate tree species. *Plant and Soil*,
815 389, 121-129.

816

817 McCormack, M. L., Guo, D., Iversen, C. M., Chen, W., Eissenstat, D. M., Fernandez, C. W., ... &
818 Zanne, A. (2017). Building a better foundation: Improving root-trait measurements to understand
819 and model plant and ecosystem processes. *New Phytologist*, 215, 27-37.

820

821 McCormack, M. L., & Iversen, C. M. (2019). Physical and functional constraints on viable
822 belowground acquisition strategies. *Frontiers in Plant Science*, 1215.

823

824 McElrone, A. J., Pockman, W. T., Martínez-Vilalta, J., & Jackson, R. B. (2004). Variation in xylem
825 structure and function in stems and roots of trees to 20 m depth. *New phytologist*, 163, 507-517.

826

827 Moorcroft, P. R., Hurtt, G. C., & Pacala, S. W. (2001). A method for scaling vegetation dynamics:
828 the ecosystem demography model (ED). *Ecological Monographs*, 71, 557-586.

829

830 Nara, K. (2006). Ectomycorrhizal networks and seedling establishment during early primary
831 succession. *New Phytologist*, 169, 169-178.

832

833 Norman, J.M., 1993. Scaling processes between leaf and canopy levels. In: Ehleringer, J. R., Field,
834 C.B. (Eds.), *Scaling Physiological Processes: Leaf to Globe*. Academic Press, New York, pp. 41–
835 76.

836

837 O'Brien, A. M., Ginnan, N. A., Rebolleda-Gómez, M., & Wagner, M. R. (2021). Microbial effects
838 on plant phenology and fitness. *American Journal of Botany*, 108, 1824-1837.

839

840 Okino, M. S., & Mavrovouniotis, M. L. (1998). Simplification of mathematical models of chemical
841 reaction systems. *Chemical Reviews*, 98, 391-408.

842

843 Orwin, K. H., Kirschbaum, M. U., St John, M. G., & Dickie, I. A. (2011). Organic nutrient uptake
844 by mycorrhizal fungi enhances ecosystem carbon storage: a model-based assessment. *Ecology*
845 Letters, 14, 493-502.

846

847 Ouimette, A.P., Ollinger, S.V., Lepine, L.C. et al. (2020). Accounting for Carbon Flux to
848 Mycorrhizal Fungi May Resolve Discrepancies in Forest Carbon Budgets. *Ecosystems* 23, 715–
849 729.

850

851 Pankow, W., Boller, T., & Wiemken, A. (1991). The significance of mycorrhizas for protective
852 ecosystems. *Experientia*, 47, 391-394.

853

854 Parton, W. J., Schimel, D. S., Cole, C. V., & Ojima, D. S. (1987). Analysis of factors controlling
855 soil organic matter levels in Great Plains grasslands. *Soil Science Society of America Journal*, 51,
856 1173-1179.

857

858 Phillips, R. P., Brzostek, E., & Midgley, M. G. (2013). The mycorrhizal-associated nutrient
859 economy: a new framework for predicting carbon–nutrient couplings in temperate forests. *New*
860 *Phytologist*, 199, 41-51.

861

862 Pointurier, O., Moreau, D., Pagès, L., Caneill, J., & Colbach, N. (2021). Individual-based 3D
863 modelling of root systems in heterogeneous plant canopies at the multiannual scale. Case study
864 with a weed dynamics model. *Ecological Modelling*, 440, 109376.

865

866 Polverigiani, S., McCormack, M. L., Mueller, C. W., & Eissenstat, D. M. (2011). Growth and
867 physiology of olive pioneer and fibrous roots exposed to soil moisture deficits. *Tree Physiology*,
868 31, 1228-1237.

869

870 Pregitzer, K. S. (2002). Fine roots of trees—a new perspective. *New Phytologist*, 154, 267-270.

871

872 Pregitzer, K. S., DeForest, J. L., Burton, A. J., Allen, M. F., Ruess, R. W., & Hendrick, R. L.
873 (2002). Fine root architecture of nine North American trees. *Ecological Monographs*, 72, 293-309.

874

875 Prescott, C. E., Grayston, S. J., Helmisaari, H. S., Kaštovská, E., Körner, C., Lambers, H., ... &
876 Ostonen, I. (2020). Surplus carbon drives allocation and plant–soil interactions. *Trends in Ecology
& Evolution*, 35, 1110-1118.

877

878

879 Radville, L., McCormack, M. L., Post, E., & Eissenstat, D. M. (2016). Root phenology in a
880 changing climate. *Journal of Experimental Botany*, 67, 3617-3628.

881

882 Raunkiaer, C.C. 1934. The Life Forms of Plants and Statistical Plant Geography. Clarendon Press,
883 Oxford

884

885 Raupach, M.R., Finnigan, J.J., 1988. 'Single-layer models of evaporation from plant canopies are
886 incorrect but useful, whereas multilayer models are correct but useless'. *Discuss. Aust. Journal
887 Plant Physiol.* 15, 705–716.

888

889 Raven, J. A., & Edwards, D. (2001). Roots: evolutionary origins and biogeochemical significance.

890 *Journal of Experimental Botany*, 52, 381-401.

891

892 Read, D. J. (1991). Mycorrhizas in ecosystems. *Experientia*, 47, 376-391.

893

894 Rees, M., Condit, R., Crawley, M., Pacala, S., & Tilman, D. (2001). Long-term studies of

895 vegetation dynamics. *SCIENCE*, 293, 650-655.

896

897 Ricciuto, D., Sargsyan, K., & Thornton, P. (2018). The impact of parametric uncertainties on

898 biogeochemistry in the E3SM land model. *Journal of Advances in Modeling Earth Systems*, 10,

899 297–319.

900

901 Robin, A., Pradier, C., Sanguin, H. et al. (2019). How deep can ectomycorrhizas go? A case study

902 on *Pisolithus* down to 4 meters in a Brazilian eucalypt plantation. *Mycorrhiza* 29, 637–648.

903

904 Root, R. B. (1967). The niche exploitation pattern of the blue-gray gnatcatcher. *Ecological*

905 *Monographs* 37, 317–350.

906

907 Sauter, F., Albrecht, H., Kollmann, J., & Lang, M. (2021). Competition components along

908 productivity gradients—revisiting a classic dispute in ecology. *Oikos*. 130, 1326-1334.

909

910 Sellers, P. J., Mintz, Y. C. S. Y., Sud, Y. E. A., & Dalcher, A. (1986). A simple biosphere model

911 (SiB) for use within general circulation models. *Journal of the Atmospheric Sciences*, 43, 505-531.

912

913 Sen, D. N., & Jenik, J. (1962). Root ecology of *Tilia europaea* L.: anatomy of Mycorrhizal roots.

914 Nature, 193, 1101-1102.

915

916 Shugart, H. H. A Theory of Forest Dynamics (Springer, 1984).

917

918 Shugart, H. H., Wang, B., Fischer, R., Ma, J., Fang, J., Yan, X., ... & Armstrong, A. H. (2018).

919 Gap models and their individual-based relatives in the assessment of the consequences of global

920 change. Environmental Research Letters, 13, 033001.

921

922 Sinclair, T.R., Murphy, C.E., Knoerr, K.R., 1976. Development and evaluation of simplified

923 models for simulating canopy photosynthesis and transpiration. J. Appl. Ecol 13, 813–829.

924

925 Smith et al. Plant Functional Types: Their Relevance to Ecosystem Properties and Global Change.

926 (1997). United Kingdom: Cambridge University Press.

927

928 Smithwick, E. A., Lucash, M. S., McCormack, M. L., & Sivandran, G. (2014). Improving the

929 representation of roots in terrestrial models. Ecological Modelling, 291, 193-204.

930

931 Sousa, D., Fisher, J. B., Galvan, F. R., Pavlick, R. P., Cordell, S., Giambelluca, T. W., et al. (2021).

932 Tree canopies reflect mycorrhizal composition. Geophysical Research Letters, 48,

933 e2021GL092764.

934

935 Steinaker DF, Wilson SD, Peltzer DA. 2010. Asynchronicity in root and shoot phenology in
936 grasses and woody plants. *Global Change Biology* 16, 2241–2251.

937

938 Stone, E. L., & Kalisz, P. J. (1991). On the maximum extent of tree roots. *Forest ecology and*
939 *management*, 46, 59-102.

940

941 Sun, T., Hobbie, S. E., Berg, B., Zhang, H., Wang, Q., Wang, Z., & Hättenschwiler, S. (2018).
942 Contrasting dynamics and trait controls in first-order root compared with leaf litter decomposition.
943 *Proceedings of the National Academy of Sciences*, 115, 10392-10397.

944

945 Thornton, P. E., Lamarque, J. F., Rosenbloom, N. A., & Mahowald, N. M. (2007). Influence of
946 carbon-nitrogen cycle coupling on land model response to CO₂ fertilization and climate
947 variability. *Global biogeochemical cycles*, 21(4).

948

949 Tierney, G. L., Fahey, T. J., Groffman, P. M., Hardy, J. P., Fitzhugh, R. D., Driscoll, C. T., &
950 Yavitt, J. B. (2003). Environmental control of fine root dynamics in a northern hardwood forest.
951 *Global Change Biology*, 9, 670-679.

952

953 Transtrum, M. K., Machta, B. B., Brown, K. S., Daniels, B. C., Myers, C. R., & Sethna, J. P.
954 (2015). Perspective: Sloppiness and emergent theories in physics, biology, and beyond. *The*
955 *Journal of Chemical Physics*, 143(1), 07B201_1.

956

957 Treseder, K. K. (2016). Model behavior of arbuscular mycorrhizal fungi: predicting soil carbon
958 dynamics under climate change. *Botany*, 94, 417-423.

959

960 Tumber-Dávila, S. J., Schenk, H. J., Du, E., & Jackson, R. B. (2022). Plant sizes and shapes above
961 and belowground and their interactions with climate. *New Phytologist*, 235, 1032-1056

962

963 Wang, B., Shugart, H. H., Shuman, J. K., & Lerdau, M. T. (2016). Forests and ozone: Productivity,
964 carbon storage and feedbacks. *Scientific Reports*, 6, 1-7.

965

966 Wang, B., and Allison, S. D. (2019). Emergent properties of organic matter decomposition by soil
967 enzymes. *Soil Biology and Biochemistry*, 136, 107522.

968

969 Wang, B., and Allison, S.D. (2022). Climate-driven legacies in simulated microbial communities
970 alter litter decomposition rates. *Frontiers in Ecology and Evolution*, 10, 841824.

971

972 Wang, B., Brewer, P. E., Shugart, H. H., Lerdau, M. T., & Allison, S. D. (2019). Building bottom-
973 up aggregate-based models (ABMs) in soil systems with a view of aggregates as biogeochemical
974 reactors. *Global Change Biology*, 25, e6-e8.

975

976 Wang, Q., Zhang, Z., Zhu, X., Liu, Z., Li, N., Xiao, J., ... & Yin, H. 2022. Absorptive roots drive
977 a larger microbial carbon pump efficacy than transport roots in alpine coniferous forests. *Journal*
978 of Ecology. <https://doi.org/10.1111/1365-2745.13899>

979

980 Warren JM, Bilheux H, Kang M, Voisin S, Cheng C-L, Horita J, Perfect E. 2013. Neutron imaging
981 reveals internal plant water dynamics. *Plant and Soil* 366, 683–693.

982

983 Warren, J. M., Hanson, P. J., Iversen, C. M., Kumar, J., Walker, A. P., & Wullschleger, S. D.
984 (2015). Root structural and functional dynamics in terrestrial biosphere models—evaluation and
985 recommendations. *New Phytologist*, 205, 59-78.

986

987 Watt, A. S. (1947). Pattern and process in the plant community. *Journal of Ecology*, 35, 1-22.

988

989 Weigelt, A., Mommer, L., Andraczek, K., Iversen, C. M., Bergmann, J., Bruelheide, H., ... &
990 McCormack, M. L. (2021). An integrated framework of plant form and function: The belowground
991 perspective. *New Phytologist*, 232, 42-59.

992

993 We must get a grip on forest science—before it's too late. (2022). *Nature* 608, 449.

994 <https://doi.org/10.1038/d41586-022-02182-0>

995

996 Wieder, W. R., Grandy, A. S., Kallenbach, C. M., Taylor, P. G., & Bonan, G. B. (2015).
997 Representing life in the Earth system with soil microbial functional traits in the MIMICS model.
998 *Geoscientific Model Development*, 8, 1789-1808.

999

1000 Woodward, F. I., & Smith, T. M. (1994). Global photosynthesis and stomatal conductance:
1001 Modelling the controls by soil and climate. In *Advances in Botanical Research* (Vol. 20, pp. 1-41).
1002 Academic Press.

1003

1004 Yan, H., Wang, S. Q., Yu, K. L., Wang, B., Yu, Q., Bohrer, G., ... & Shugart, H. H. (2017). A
1005 novel diffuse fraction-based two-leaf light use efficiency model: An application quantifying
1006 photosynthetic seasonality across 20 AmeriFlux flux tower sites. *Journal of Advances in Modeling
1007 Earth Systems*, 9, 2317-2332.

1008

1009 Yang, X., Ricciuto, D. M., Thornton, P. E., Shi, X., Xu, M., Hoffman, F., & Norby, R. J. (2019).
1010 The effects of phosphorus cycle dynamics on carbon sources and sinks in the amazon region: a
1011 modeling study using ELM v1. *Journal of Geophysical Research: Biogeosciences*, 124, 3686-
1012 3698.

1013

1014 Yang, X., Thornton, P. E., Ricciuto, D. M., & Post, W. M. (2014). The role of phosphorus
1015 dynamics in tropical forests—a modeling study using CLM-CNP. *Biogeosciences*, 11, 1667-1681.

1016

1017 Zanne, A. E., Abarenkov, K., Afkhami, M. E., Aguilar-Trigueros, C. A., Bates, S., Bhatnagar, J.
1018 M., ... & Treseder, K. K. (2020). Fungal functional ecology: bringing a trait-based approach to
1019 plant-associated fungi. *Biological Reviews*, 95, 409-433.

1020

1021 Zeng, X. (2001). Global vegetation root distribution for land modeling. *Journal of
1022 Hydrometeorology*, 2, 525-530.

1023

1024 Zhou, M., Guo, Y., Sheng, J., Yuan, Y., Zhang, W. H., & Bai, W. (2022). Using anatomical traits
1025 to understand root functions across root orders of herbaceous species in temperate steppe. *New
1026 Phytologist*. <https://doi.org/10.1111/nph.17978>

1027

1028 Zhu, Q., W. J. Riley, and J.Y. Tang (2017) A new theory of plant–microbe nutrient competition
1029 resolves inconsistencies between observations and model predictions, *Ecological Applications*, 27,
1030 875–886

1031

Appendix

1032

1033 **Embracing fine-root system complexity to improve the predictive understanding of** 1034 **ecosystem functioning**

1035

1036

1037 1. Methods

1038 1.1 Simple ELM (sELM)

1039 sELM is a simplified version of the Energy Exascale Earth System Model (E3SM) Land
1040 Model ELM, a state-of-the-art land surface model developed by Department of Energy, United
1041 States (**Golaz et al. 2019; Burrows et al. 2020**). ELM is traced back to the original CLM4.5
1042 (**Oleson et al. 2013**) and the later version E3SM Land Model (ELM). sELM simplifies ELM by
1043 keeping only essential components simulating natural ecosystems in North America including
1044 vegetation and soil biogeochemistry (**Lu and Ricciuto 2019**). Following the same global PFT
1045 classification scheme as ELM, vegetation has the same structural pools (with a single fine-root
1046 pool) as ELM using the big-leaf approach. Although photosynthesis and GPP are replaced by a
1047 neural network surrogate built from ELM simulations, the whole scheme of allocation of
1048 photosynthates remains the same. Soil system, except for the lack of hydrology, is the same as the
1049 ELM with a 10-layer profile of 3.8018 m deep. Litter and soil organic matter decomposition follow
1050 the CTC (Converging Trophic Cascade) framework (**Oleson et al. 2013; Burrows et al. 2020**).
1051 Plant-microbe competition for mineral nitrogen is achieved via the relative demand approach
1052 without further differentiating between nitrogen forms (i.e., NH₄ and NO₃). Such a simplified
1053 model, in a more formal sense, is a high-fidelity mechanistic surrogate; by omitting irrelevant

1054 processes but keeping all essential components, it eases modifications of structures and processes
1055 and reduces computational burden for analyses of uncertainty and sensitivity, contributing to an
1056 acceleration of the development-evaluation-application cycle for Earth System Models in
1057 particular.

1058

1059 **1.2 Realization of TAM**

1060 **1.2.1 Partitioning**

1061 We directly introduce three parameters (*frootpar_i*, where *i* indexes the three fine root pools
1062 of T, A, and M) to determine the spreading of allocation to a fine-root system (from either
1063 photosynthates or storage) among TAM pools. This approach simplifies the partitioning without
1064 considering explicitly the processes of movement of carbohydrates across the branching structure.
1065 With known partitioning (*frootpar_i*) and fine root C/N (*frootcn_i*), allocation allometry (ratio of
1066 allocation to total new growth to allocation to new leaf, *Callom/Nallom*) can be determined
1067 following:

1068

$$1069 \begin{cases} Callom = (1 + g1)[1 + a1 + a3(1 + a2)] \\ Nallom = \frac{1}{CN_{leaf}} + a1 \sum_{i=1}^3 \frac{frootpar_i}{frootcn_i} + \frac{a3a4(1+a2)}{CN_{livewood}} + \frac{a3(1-a4)(1+a2)}{CN_{deadwood}} \end{cases} \quad (1)$$

1070

1071 where **a1** through **a4** are allometric parameters that relate allocation between various tissue types,
1072 among which **a1** is the ratio of new fine root to new leaf carbon allocation (i.e., *froot_leaf*), **a2**
1073 ratio of new coarse root to new stem carbon allocation, **a3** ratio of new stem to new leaf carbon
1074 allocation, **a4** ratio new live wood to new total wood allocation, and **g1** allocation ratio of growth
1075 respiration carbon to new growth carbon, as well as C/N of both live wood and dead wood. TAM

1076 pools are parameterized with different C/N ratios based on consistent observations of descending
1077 C/N while fine-root systems branching out (e.g., **Pregitzer et al. 1997; McCormack et al. 2015**).

1078
1079 **1.2.2 Phenology**

1080 In ELM, fine-root production is temporally controlled by leaf phenology in moving carbon
1081 from two direct sources: recent photosynthate and storage, making leaf and root production
1082 perfectly synchronous. These two sources, though ultimately originating from photosynthesis, can
1083 also be referred to as direct and indirect allocation, respectively. The allocation from leaf
1084 photosynthates to the fine-root system is based on an allometric relationship between leaves and
1085 fine roots ($froot_leaf = 1$). This allocation is divided between direct allocation to the currently
1086 displayed fine-root system ($fcur$) and a storage pool to supply future growth for the whole fine-
1087 root system (i.e., indirect allocation; $1 - fcur$). This storage-based indirect allocation is also
1088 controlled by leaf phenology. Such a totally synchronous treatment between leaf and fine-root
1089 production is the case across all current ecosystem models, which, however, does not reflect the
1090 increasingly rich evidence that shoot and root phenology are not synchronous (e.g., **Perry 1971**;
1091 **Steinaker and Wilson 2008; Steinaker et al. 2010; McCormack et al. 2015b; Abramoff &**
1092 **Finzi 2015; Radville et al. 2016**). We make the following 3-step changes to decouple the
1093 phenological control of shoot and TAM in both deciduous and evergreen systems.

1094 First, we make evergreen PFTs have the two-source structure of storage and recent
1095 photosynthate. In the current ELM, this two-source structure only applies to deciduous PFTs.
1096 Evergreen PFTs do not accumulate carbon and nitrogen in the storage pools for fine-root systems;
1097 instead, root production is solely determined by direct allocation of new photosynthates (i.e., $fcur$
1098 = 1), an assumption that lacks empirical support (e.g., **Huang et al. 2021**). Therefore, this
1099 treatment is changed for evergreen PFTs to have the same two-source structure as deciduous PFTs.

1100 This structure enables storage-based production of (or indirect allocation to) fine-root systems
1101 controlled by TAM phenology.

1102 Then, we decouple TAM phenology from leaf phenology for both deciduous and evergreen
1103 PFTs (Fig.1). In the current ELM, storage-based initiation of fine roots is synchronous with leaf-
1104 based control of unfolding (triggered by a growing degree threshold) and shedding (triggered by a
1105 critical day length). This synchronous treatment is changed to allow TAM initiation to behave
1106 independently in both deciduous and evergreen systems, which are determined by **GDDsum**
1107 (growing degree days with a 0-degree base) relative to a threshold value, **GDDfroot_sum_crit**:

1108

$$1109 GDD_{froot_sum_crit} = GDD_{leaf_sum_crit} + \Delta GDD_{froot_leaf} \quad (2)$$

1110

1111 where ΔGDD_{leaf_froot} is the difference between leaf and fine root threshold of GDD. Once
1112 $GDDsum > GDD_{froot_sum_crit}$, TAM initiation is triggered, and fluxes of carbon and nitrogen
1113 begin to move from storage pools (CS_{froot_stor}) to the fine-root system. This occurs via transfer
1114 pools ($CF_{froot_stor,froot_xfer}$) calculated following:

1115

$$1116 CF_{froot_stor,froot_xfer} = f_{stor,xfer} CS_{froot_stor} \quad (3)$$

1117

1118 where $f_{stor,xfer} = 0.5$, the fraction of current storage pool moved into the transfer pool for display
1119 over the incipient onset period (Oleson et al. 2013).

1120 Finally, we make TAM turnover of deciduous PFTs dependent on pool-specific mortality.
1121 For deciduous PFTs in the current ELM, the shedding of fine roots is synchronous with leaf
1122 shedding, which lacks empirical support. This synchronous treatment is thus changed to allow

1123 deciduous fine-root mortality to behave independently in deciduous systems in the same way as
1124 the fine roots of evergreen PFTs. See **Section 1.2.4** on TAM mortality.

1125

1126 **1.2.3 Distribution**

1127 In ELM and other land surface models, the prevailing option assumes that fine roots and
1128 coarse roots follow the same distribution as determined by prescribed fixed rooting and soil depths
1129 following:

1130

1131 $r_{croot_i} =$

$$1132 \begin{cases} 0.5[\exp(-r_a z_{h,i-1}) + \exp(-r_b z_{h,i-1}) - \exp(-r_a z_{h,i}) - \exp(-r_b z_{h,i})], & \text{for } 1 \leq i < N_{levsoi} \\ 0.5[\exp(-r_a z_{h,i-1}) + \exp(-r_b z_{h,i-1})], & \text{for } i = N_{levsoi} \end{cases} \quad (4)$$

1133)

1134

1135 where **ra** and **rb** are PFT-dependent root distribution parameters. Because of the dynamic nature
1136 of fine-root systems, the vertical profile is modelled dynamically by assuming horizontal
1137 homogenization of TAM (that is, the same distribution profile across T, A, and M) constrained by
1138 nutrient and water availability:

1139

$$1140 r_{froot_i} = \frac{r_{croot_i} f_{n_i} f_{m_i}}{\sum_{i=1}^{N_{levsoi}} r_{croot_i} f_{n_i} f_{m_i}} \quad (5)$$

1141

1142 where **fn_i** and **fm_i** are the relative availability of nutrients and the relative availability of water
1143 at soil layer i, respectively. This nutrient constraint means that relatively more of the allocation
1144 goes to the depth where the relative nutrient availability is high; that is, a plant can direct allocation

1145 and distribution to the place where the nutrients are relatively richer. Note that root-water
1146 interactions are beyond the scope of this study and are not included in the analysis below. Such a
1147 realization of a dynamic profile contingent on a fixed coarse root profile partly accounts for the
1148 notion that coarser roots provide a structural constraint for potential fine-root system distribution
1149 dictated by the hierarchical branching structure of root systems.

1150

1151 1.2.4 Mortality and litter input

1152 With a 3-pool structure, turnover of the fine-root system is modelled explicitly in a
1153 vertically resolved way by introducing a mortality term. Mortality of fine roots and mycorrhizal
1154 fungi is endogenously controlled but subject to exogenous influences (e.g., **Eissenstat & Yanai**
1155 **1997; Hendrick and Pregitzer 1997**). Therefore, consistent with the current approach in ELM
1156 modelling turnover using a mortality parameter in general, TAM mortality in each time step is
1157 determined by longevity distinguished among T, A, and M (*froot_long*) and constrained by a
1158 depth-correction term (α) as follows:

1159

$$1160 \left\{ \begin{array}{l} Mr_{i,j} = \frac{1}{froot_long_i} \alpha_j \\ \alpha_j = e^{-\frac{dz_j}{mort_depth_efolding}} \end{array} \right. \quad (6)$$

1161

1162 where *froot_long_i* is longevity of the three TAM pools near the soil surface,
1163 *mort_depth_efolding* is a constant of mortality rate decrease with depth, and *dzj* is depth of soil
1164 layer *j*.

1165 Mortality of the T, A, and M pools are parameterized with different but decreasing
1166 lifespans based on relatively easy-to-make observations in shallow soil depths (**Supplementary**

1167 **Table 1**). This pattern is based on field observations of a dramatic increase in survivorship with
1168 diameter even within a very narrow range (e.g., ≤ 0.5 mm) (e.g., **Reid et al., 1993; Hendrick &**
1169 **Pregitzer 1993; Tierney & Fahey 2002; Edwards et al. 2004; Joslin et al. 2006; Espeleta et al.**
1170 **2009; Riley et al. 2009; Xia et al. 2010**) and direct observations of lifespan and turnover in fungal
1171 tissues (**Allen and Kitajima 2013; McCormack et al. 2010**). The depth-correction term (α)
1172 further corrects the fine root and fungi longevity (*froot_long*) for increasing lifespan with soil
1173 depth (e.g., **Baddeley and Waston 2005; Iversen et al. 2008; McCormack et al. 2012; Germon**
1174 **et al 2015; Gu et al. 2017**). This depth-based correction partly accounts for the plasticity of fine-
1175 root systems in response to vertical variability in soil resource availability (e.g., **Pregitzer et al.**
1176 **1993; Eissenstat and Yanai, 1997**).

1177 An explicit turnover of fine-root systems means explicit production of litters from the three
1178 pools. The TAM structure is coupled with existing litter decomposition model simply by
1179 aggregating litters across the 3 pools and depositing them in the three vertically resolved soil litter
1180 pools—labile, cellulose/hemicellulose, and lignin (**Oleson et al. 2013**). Each of the three fine-root
1181 pools is parameterized with fractions of these three different groups in terms of C (**Supplementary**
1182 **Table 1**). Nitrogen fluxes to the three litter pools from each of the three fine root pools are
1183 determined using the same fractions as used for carbon fluxes and their C/N ratios.

1184 Additionally, maintenance and growth respiration follow the current ELM implementation
1185 (**Oleson et al. 2013**). Maintenance respiration rate is related to temperature and tissue N content
1186 without further differentiating intrinsic respiration rate and temperature sensitivity among TAM
1187 roots; varying N content differentiates respiration among TAM roots. Growth respiration is still
1188 calculated as a factor of 0.3 (*grperc*) times the total carbon in new growth including the fine-root
1189 system.

1190

1191 **1.3 Parameterization and simulation**

1192 We implemented the changes as detailed above to realize the TAM structure in sELM. This
1193 implementation is referred to as TAM model (or TAM in short), while the original version is
1194 referred to as ELM. For an illustration purpose, we parameterized TAM and ELM for 2 temperate
1195 forests across the East US: Howland Forest (<https://ameriflux.lbl.gov/sites/siteinfo/US-Ho1>);
1196 **Hollinger et al. 2021**; a single temperate evergreen needleleaf PFT) and Ozark
1197 (<https://ameriflux.lbl.gov/sites/siteinfo/US-MOz>; a single temperate deciduous broadleaf PFT; **Gu**
1198 **et al. 2016**). We used FRED (v3.0), a global Fine-Root Ecology Database to address below-ground
1199 challenges in plant ecology (<https://roots.ornl.gov/>; **Iversen et al. 2017**; **Iversen and McCormack**
1200 **2021**), FunFun, a fungal trait database (**Zanne et al. 2020**), and published literature to derive PFT-
1201 specific parameter values/ranges for TAM (**Supplementary Table 1**). Simulation at each site was
1202 driven by forcings including daily radiation, maximum and minimum temperature, precipitation,
1203 day length, and a constant CO₂ level (cycled 6 times).

1204

1205 **1.4 Uncertainty and sensitivity analysis**

1206 TAM was compared with ELM (with default parameterization) by accounting for structural
1207 and parameter uncertainties introduced by the novel 3-pool structure. These comparisons involved
1208 outputs of interest including fluxes of GPP and heterotrophic respiration and pools of leaf and fine-
1209 root system TAM, as well as the nitrogen limitation factors for plant growth (i.e., Fraction of
1210 Potential Growth, $FPG = F_{plant_uptake}/F_{plant_demand}$).

1211 First, one case of preserving the fine-root system C/N of ELM in TAM was examined to
1212 see impacts of this structural shift and its associated uncertainties. To preserve the fine-root system

1213 C/N in TAM (i.e., the default parameterization of C/N = 42), two specific scenarios were derived
1214 by solving the following equation, **Eq.7**, conditioned on the observed pattern of ascending C/N
1215 across the hierarchical branching orders within fine-root systems (e.g., **McCormack et al. 2015a**)
1216 and on prescribing one case of descending allocation from T through A (**TAM_descend**) and one
1217 case of ascending allocation (**TAM_ascend**):

1218

$$1219 \left\{ \begin{array}{l} \sum_{i=1}^3 \frac{frootcn_i}{frootpar_i} = 42 \\ frootcn_t > frootcn_a > frootcn_m \\ frootpar_i = [0.5, 0.3, 0.2] \text{ or } [0.2, 0.3, 0.5] \end{array} \right. \quad (7)$$

1220

1221 By prescribing two alternatives of partitioning fraction vector, the equation has two corresponding
1222 closed solutions of **frootcn_i**: [60,42,24] or [72,42,36]. In other words, by preserving the fine-root
1223 system C/N and keeping the same phenology and distribution between ELM and TAM, the
1224 uncertainty of the TAM structure for these two scenarios potentially arose from parameters of only
1225 chemistry and longevity. On top of these two cases, a structural uncertainty arising from nitrogen-
1226 constrained dynamic vertical distribution of new allocation was also examined, which were
1227 referred to as **TAM_descend_dd** and **TAM_ascend_dd**, respectively.

1228 Next, without preserving the C/N ratio, a full implementation of TAM (including
1229 phenology) was compared with ELM. This comparison, relative to the above case, accounted for
1230 uncertainty arising from parameters including C/N and partitioning (6 parameters) and phenology-
1231 related parameters [3 parameters: **gdd_crit** (for evergreen PFT only), **gdd_crit_gap**, **fcur**]
1232 (**Supplementary Table 1**). That is, varying the partitioning and C/N parameters freely and
1233 phenology-related parameters under a full implementation of the proposed implementation of

1234 TAM, changes relative to ELM and their uncertainty were attributed to these newly introduced
1235 parameters.

1236 Finally, a global sensitivity analysis of TAM was performed with 8 (7 for evergreen PFT
1237 which does not have *crit_dayl*) more existing parameters in ELM (**Supplementary Table 2**). All
1238 parameter uncertainty was quantified by 1080 ensemble runs from Monte-Carlo sampling from
1239 parameters' uniform uncertainty ranges and uncertainty propagation through the model.
1240 Attribution of TAM uncertainty was then achieved via variance-based sensitivity analysis with
1241 Sobol's sensitivity indices (**Sobol 2003; Ricciuto et al. 2018**). The Sobol's sensitivity indices were
1242 indirectly derived from a polynomial chaos expansion of the outputs via a new Weighted Iterative
1243 Bayesian Compressive Sensing (WIBCS) algorithm using the Uncertainty Quantification Toolkit
1244 (**UQTk v3.0.2**; <https://github.com/sandialabs/UQTk>).

1245

Supplementary Table 1. List of introduced parameters and their uncertainty ranges.

Parameter	Description	Unit	Range(evergreen/deciduous)	Reference
<i>frootcn_t</i>	C/N of T root	-	[20,184]/[19, 116]	FRED v3
<i>frootcn_a</i>	C/N of A root	-	[11,119]/[9, 81]	FRED v3
<i>frootcn_m</i>	C/N of M root	-	[7,25]/[7, 25]	Zanne et al. 2019
<i>frootpar_t</i>	Fraction of total allocation to T	-	[0.05, 0.95]	
<i>frootpar_a</i>	Fraction to total allocation to A	-	[0.05, 0.95]	
<i>frootpar_m</i>	Fraction to total allocation to M	-	[0.05, 0.95]	
<i>frootlong_t</i>	Longevity of T	year	[3, 10]	Matamala et al. 2003; Xia et al. 2010
<i>frootlong_a</i>	Longevity of A	year	[0.5, 4]	Matamala et al. 2003; Xia et al. 2010
<i>frootlong_m</i>	Longevity of M	year	[0.13, 1]	Pepe et al. 2018
<i>fr_flab_t</i>	Fraction of labile carbon in T	-	[0.125, 0.375]	± 50% of default value
<i>fr_flab_a</i>	Fraction of labile carbon in A	-	[0.125, 0.375]	± 50% of default value
<i>fr_flab_m</i>	Fraction of labile carbon in M	-	[0.125, 0.375]	± 50% of default value
<i>fr_flig_t</i>	Fraction of lignin carbon in T	-	[0.125, 0.375]	± 50% of default value
<i>fr_flig_a</i>	Fraction of lignin carbon in A	-	[0.125, 0.375]	± 50% of default value
<i>fr_flig_m</i>	Fraction of lignin carbon in M	-	[0.125, 0.375]	± 50% of default value
<i>fr_fcel_t</i>	Fraction of cellulose/hemicellulose C in T	-	[0.25, 0.75]	± 50% of default value
<i>fr_fcel_a</i>	Fraction of cellulose/hemicellulose C in A	-	[0.25, 0.75]	± 50% of default value
<i>fr_fcel_m</i>	Fraction of cellulose/hemicellulose C in M	-	[0.25, 0.75]	± 50% of default value
<i>mort_depth_efolding</i>	Rate of mortality decrease with depth	-	[187.15e-3,935.75e-3]	Iversen et al. 2008; McCormack et al. 2012; Germon et al 2015; Gu et al. 2017
<i>gdd_crit_gap</i>	Difference in GDD between root and leaf onset	°C *day	[-300, 300]	Expert judgement

1246

1247

Supplementary Table 2. List of existing parameters of interest in ELM and their uncertainty ranges.

Parameter	Description	Unit	Range(evergreen/deciduous)
<i>gdd_crit</i>	Leaf onset GDD	°C *day	150, 750
<i>fcur</i>	fraction of root allocation to display in current time step	-	[0.5, 1.0]/[0, 1]
<i>froot_leaf</i>	ratio of new fine root to new leaf carbon allocation	-	[0.5, 1.5]
<i>slatop</i>	Specific leaf area at canopy top	m ² gC ⁻¹	[0.005,0.015]/[0.015,0.045]
<i>crit_dayl</i>	Critical day length for leaf senescence in deciduous	Seconds	[36000, 43000]
<i>leafcn</i>	leaf C/N	-	[17.5, 52.5]/[12.5, 37.5]
<i>roota_par</i>	Rooting depth distribution parameter	m ⁻¹	[1.5,4.5]/[3, 9]
<i>rootb_par</i>	Rooting depth distribution parameter	m ⁻¹	[0.625, 1.875]/[1, 3]
<i>br_mr</i>	Base rate for maintenance respiration (MR)	umol m ⁻² s ⁻¹	[1.26e-06, 3.78e-06]
<i>q10_mr</i>	Temperature sensitivity for MR	-	[0.75, 2.25]

1248

1249

1250

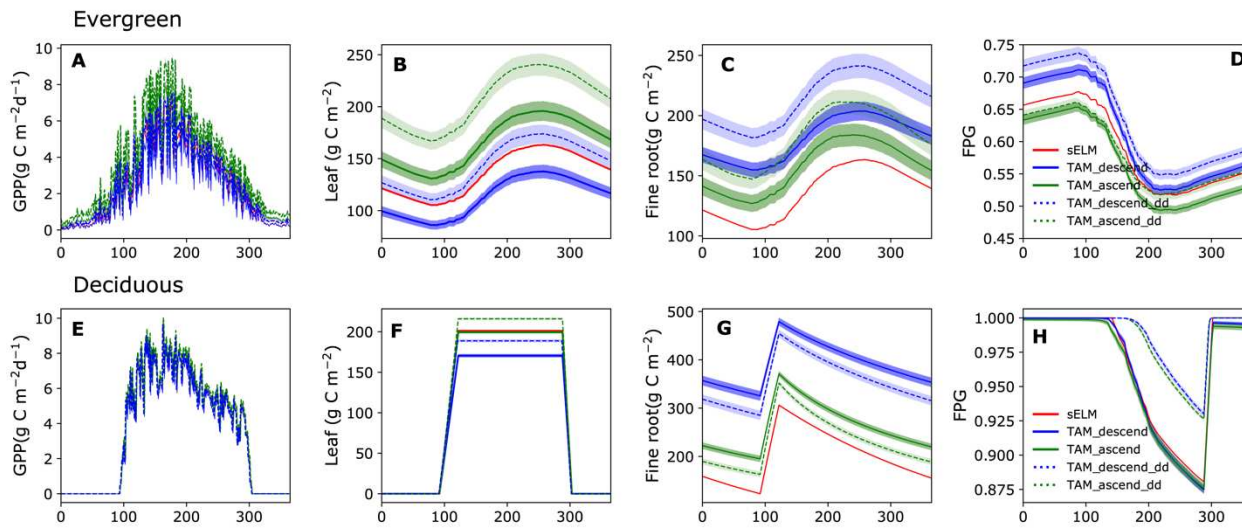
1251

1252

1253

1254 **2. Results**

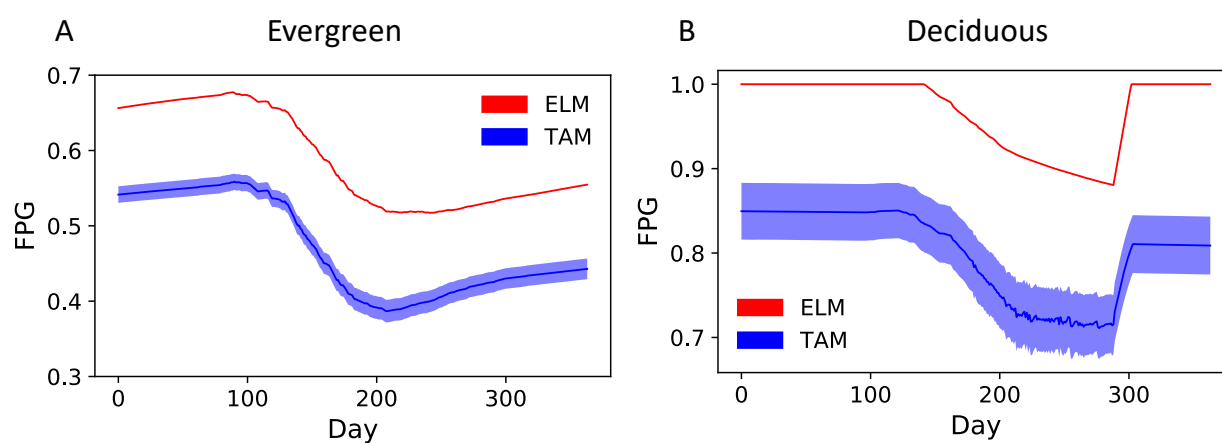
1255



1257 **Supplementary Fig. 1** Seasonal dynamics of GPP, leaf mass, and fine-root mass, as well as FPG
1258 (Fraction of Potential Growth) of TAM against the 1-pool structure of sELM under preservation
1259 of bulk fine-root system stoichiometry.

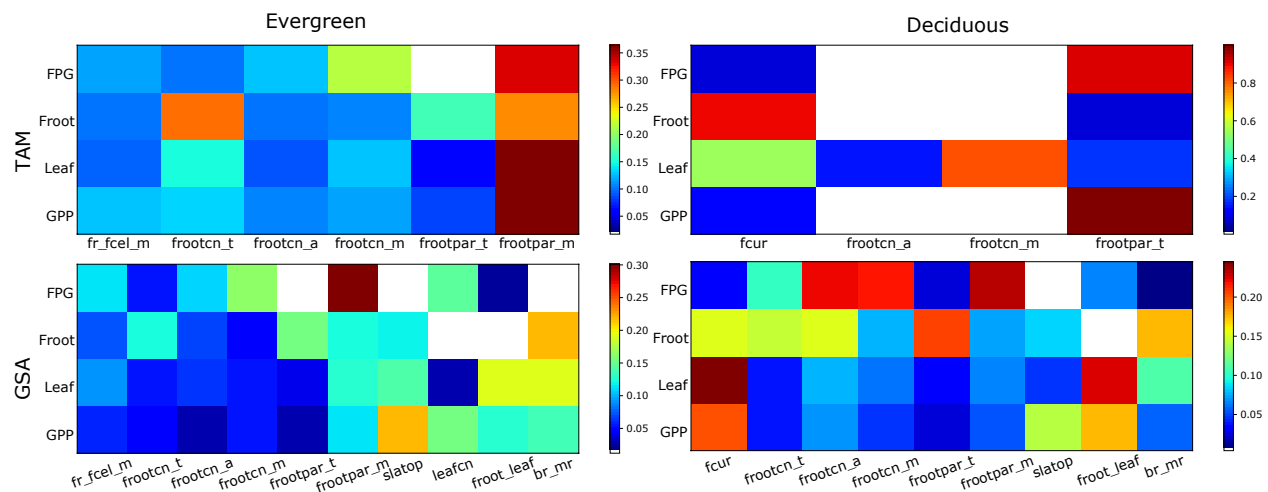
1260

1261



1263 **Supplementary Fig. 2** Seasonal variation in FPG (Fraction of Potential Growth) under a full
1264 implementation of TAM corresponding to **Fig.4** in the main text.

1265



1266

1267 **Supplementary Fig. 3 Attribution of TAM and global uncertainty with the main effect**
1268 **sensitivity index for the two sites.** The TAM sensitivity corresponds to **Fig.3** in the main text.
1269 The global sensitivity analysis also includes some of existing parameters (**Supplementary Table**
1270 **2**). Only the most relevant input parameters for each forest site are shown. The color code for each
1271 row is scaled according to the highest contributor to improve visibility.

1272

1273 **References**

1274 Abramoff, R. Z., & Finzi, A. C. (2015). Are above-and below-ground phenology in sync? *New*
1275 *Phytologist*, 205, 1054-1061.

1276

1277 Allen, M. F., & Kitajima, K. (2013). In situ high-frequency observations of mycorrhizas. *New*
1278 *Phytologist*, 200, 222-228.

1279

1280 Baddeley, J. A., & Watson, C. A. (2005). Influences of root diameter, tree age, soil depth and
1281 season on fine root survivorship in *Prunus avium*. *Plant and Soil*, 276, 15-22.

1282

1283 Burrows, S. M., Maltrud, M., Yang, X., Zhu, Q., Jeffery, N., Shi, X., ... & Leung, L. R. (2020).
1284 The DOE E3SM v1.1 biogeochemistry configuration: Description and simulated ecosystem-
1285 climate responses to historical changes in forcing. *Journal of Advances in Modeling Earth
1286 Systems*, 12, e2019MS001766.

1287

1288 Edwards, E. J., Benham, D. G., Marland, L. A., & Fitter, A. H. (2004). Root production is
1289 determined by radiation flux in a temperate grassland community. *Global Change Biology* 10,
1290 209-227.

1291

1292 Eissenstat, D. M., & Yanai, R. D. (1997). The ecology of root lifespan. *Advances in Ecological
1293 Research* 27, 1-60.

1294

1295 Espeleta, J. F., West, J. B., & Donovan, L. A. (2009). Tree species fine-root demography parallels
1296 habitat specialization across a sandhill soil resource gradient. *Ecology* 90, 1773-1787.

1297

1298 Germon, A., Cardinael, R., Prieto, I. et al. (2016). Unexpected phenology and lifespan of shallow
1299 and deep fine roots of walnut trees grown in a silvoarable Mediterranean agroforestry system. *Plant
1300 Soil* 401, 409–426.

1301

1302 Golaz, J.-C., Caldwell, P. M., Van Roekel, L. P., Petersen, M. R., Tang, Q., Wolfe, J. D., et al.
1303 (2019). The DOE E3SM coupled model version 1: Overview and evaluation at standard resolution.
1304 *Journal of Advances in Modeling Earth Systems*, 11, 2089–2129.

1305

1306 Gu, L., Pallardy, S. G., Yang, B., Hosman, K. P., Mao, J., Ricciuto, D., ... & Sun, Y. (2016).
1307 Testing a land model in ecosystem functional space via a comparison of observed and modeled
1308 ecosystem flux responses to precipitation regimes and associated stresses in a Central US Forest.
1309 Journal of Geophysical Research: Biogeosciences 121, 1884-1902.

1310

1311 Gu, J., Wang, Y., Fahey, T.J. et al. (2017). Effects of root diameter, branch order, soil depth and
1312 season of birth on fine root life span in five temperate tree species. European Journal of Forest
1313 Research 136, 727-738.

1314

1315 Hendrick, R. L., & Pregitzer, K. S. (1993). Patterns of fine root mortality in two sugar maple
1316 forests. Nature 361, 59-61.

1317

1318 Hendrick, R. L., & Pregitzer, K. S. (1997). The relationship between fine root demography and
1319 the soil environment in northern hardwood forests. Ecoscience, 4, 99-105.

1320

1321 Hollinger, D. Y., Davidson, E. A., Fraver, S., Hughes, H., Lee, J. T., Richardson, A. D., ... & Teets,
1322 A. Multi-Decadal Carbon Cycle Measurements Indicate Resistance to External Drivers of Change
1323 at the Howland Forest AmeriFlux Site. Journal of Geophysical Research: Biogeosciences
1324 e2021JG006276.

1325

1326 Huang, J., Hammerbacher, A., Gershenson, J., van Dam, N. M., Sala, A., McDowell, N. G., ... &

1327 Hartmann, H. (2021). Storage of carbon reserves in spruce trees is prioritized over growth in the

1328 face of carbon limitation. *Proceedings of the National Academy of Sciences* 118, e2023297118

1329

1330 Iversen, C. M., Ledford, J., & Norby, R. J. (2008). CO₂ enrichment increases carbon and nitrogen

1331 input from fine roots in a deciduous forest. *New Phytologist*, 179, 837-847.

1332

1333 Iversen, C. M. et al. (2017). A global Fine-Root Ecology Database to address below-ground

1334 challenges in plant ecology. *New Phytologist*, 215, 15–26.

1335

1336 Joslin, J. D., Gaudinski, J. B., Torn, M. S., Riley, W. J., & Hanson, P. J. (2006). Fine-root turnover

1337 patterns and their relationship to root diameter and soil depth in a ¹⁴C-labeled hardwood forest.

1338 *New Phytologist*, 172, 523-535.

1339

1340 Levine, E. R., Knox, R. G., & Lawrence, W. T. (1994). Relationships between soil properties and

1341 vegetation at the Northern Experimental Forest, Howland, Maine. *Remote Sensing of Environment*

1342 47, 231-241.

1343

1344 Lu, D. and Ricciuto, D. (2019) Efficient surrogate modeling methods for large-scale Earth system

1345 models based on machine-learning techniques. *Geoscientific Model Development* 12, 1791-1807

1346

1347 McCormack, M. L., Pritchard, S. G., Breland, S., Davis, M. A., Prior, S. A., Brett Runion, G., ...

1348 & Rogers, H. H. (2010). Soil fungi respond more strongly than fine roots to elevated CO₂ in a

1349 model regenerating longleaf pine-wiregrass ecosystem. *Ecosystems*, 13, 901-916.

1350

1351 McCormack, M.L., Adams, T. S., Smithwick, E. A., & Eissenstat, D. M. (2012). Predicting fine

1352 root lifespan from plant functional traits in temperate trees. *New Phytologist* 195, 823-831.

1353

1354 McCormack, M. L., I. A. Dickie, D. M. Eissenstat, T. J. Fahey, C. W. Fernandez, D. Guo, H.-S.

1355 Helmisaari, E. A. Hobbie, C. M. Iversen, R. B. Jackson, J. Leppälämmi-Kujansuu, R. J. Norby, R.

1356 P. Phillips, K. S. Pregitzer, S. G. Pritchard, B. Rewald, M. Zadworny (2015a). Redefining fine

1357 roots improves understanding of below-ground contributions to terrestrial biosphere processes.

1358 *New Phytologist*. 207, 505–518.

1359

1360 McCormack, M. L., Gaines, K. P., Pastore, M., & Eissenstat, D. M. (2015b). Early season root

1361 production in relation to leaf production among six diverse temperate tree species. *Plant and Soil*,

1362 389, 121-129.

1363

1364 Oleson, K., Lawrence, D., Bonan, G., Drewniak, B., Huang, M., Koven, C., ... & Yang, Z. (2013).

1365 Technical description of version 4.5 of the Community Land Model (CLM), NCAR. National

1366 Center for Atmospheric Research (NCAR) Boulder, Colorado.

1367

1368 Perry, T. O. (1971). Dormancy of Trees in Winter: Photoperiod is only one of the variables which

1369 interact to control leaf fall and other dormancy phenomena. *Science*, 171, 29-36.

1370

1371 Pregitzer, K. S., Kubiske, M. E., Yu, C. K., & Hendrick, R. L. (1997). Relationships among root
1372 branch order, carbon, and nitrogen in four temperate species. *Oecologia*, 111, 302-308.

1373

1374 Pregitzer, K. S., Hendrick, R. L., & Fogel, R. (1993). The demography of fine roots in response to
1375 patches of water and nitrogen. *New Phytologist*, 125, 575-580.

1376

1377 Radville, L., McCormack, M. L., Post, E., & Eissenstat, D. M. (2016). Root phenology in a
1378 changing climate. *Journal of Experimental Botany*, 67, 3617-3628.

1379

1380 Reid, J. B., Sorensen, I., & Petrie, R. A. (1993). Root demography in kiwifruit (*Actinidia*
1381 *deliciosa*). *Plant, Cell & Environment*, 16, 949-957.

1382

1383 Ricciuto, D., Sargsyan, K., & Thornton, P. (2018). The impact of parametric uncertainties on
1384 biogeochemistry in the E3SM land model. *Journal of Advances in Modeling Earth Systems*, 10,
1385 297–319.

1386

1387 Riley, W. J., Gaudinski, J. B., Torn, M. S., Joslin, J. D., & Hanson, P. J. (2009). Fine-root mortality
1388 rates in a temperate forest: estimates using radiocarbon data and numerical modeling. *New
1389 Phytologist*, 184, 387-398.

1390

1391 Sobol, I. M. (2003). Theorems and examples on high dimensional model representation. *Reliability
1392 Engineering and System Safety*, 79, 187–193.

1393

1394 Steinaker DF, Wilson SD. 2008. Phenology of fine roots and leaves in forest and grassland. *Journal*
1395 *of Ecology*, 96, 1222–1229.

1396

1397 Steinaker DF, Wilson SD, Peltzer DA. 2010. Asynchronicity in root and shoot phenology in
1398 grasses and woody plants. *Global Change Biology* 16, 2241–2251.

1399

1400 Tierney, G. L., & Fahey, T. J. (2002). Fine root turnover in a northern hardwood forest: a direct
1401 comparison of the radiocarbon and minirhizotron methods. *Canadian Journal of Forest Research*,
1402 32, 1692-1697.

1403

1404 Xia, M., Guo, D., & Pregitzer, K. S. (2010). Ephemeral root modules in *Fraxinus mandshurica*.
1405 *New Phytologist*, 188, 1065-1074.

1406

1407 Zanne, A. E., Abarenkov, K., Afkhami, M. E., Aguilar-Trigueros, C. A., Bates, S., Bhatnagar, J.
1408 M., ... & Treseder, K. K. (2020). Fungal functional ecology: bringing a trait-based approach to
1409 plant-associated fungi. *Biological Reviews* 95, 409-433.